JOHN V. RINGWOOD,
GIORGIO BACELLI, and
FRANCESCO FUSCO

Energy-Maximizing Control of Wave-Energy Converters

THE DEVELOPMENT OF CONTROL SYSTEM TECHNOLOGY TO OPTIMIZE THEIR OPERATION

With the recent sharp increases in the price of oil, issues of security of supply, and pressure to honor greenhouse gas emission limits (e.g., the Kyoto protocol), much attention has turned to renewable energy sources to fulfill future increasing energy needs. Wind energy, now a mature technology, has had considerable proliferation, with other sources, such as biomass, solar, and tidal, enjoying somewhat less deployment. Waves provide previously untapped energy potential, and wave energy has been shown to have some favorable variability properties (a perennial issue with many renewables, especially wind), especially when combined with wind energy [1].

Digital Object Identifier 10.1109/MCS.2014.2333253
Date of publication: 16 September 2014

1066-033X/14©2014IEEE

There are many new promising areas where control can make further contributions in wave-energy applications, including cooperative control of arrays of wave-energy devices.

The main reason for the lack of proliferation of wave energy is that harnessing the irregular reciprocating motion of the sea is not as straightforward as, for example, extracting energy from the wind. Wind-energy turbine design has mostly converged on a generic device form—the three-bladed horizontal axis turbine—and turbine technology and its associated control systems are well developed.

It is interesting that as solar energy is subsequently converted into wind and then waves, the power density *increases*. For example, at a latitude of 15° N (northeast trades), the solar insolation is 0.17 kW/m^2. However, the average wind generated by this solar radiation is about 20 kn (10 m/s), giving a power intensity of 0.58 kW/m^2 that, in turn, has the capability to generate waves with a power intensity of 8.42 kW/m^2 [2]. This progressive increase in energy intensity can be attributed to the time integration of the primary driving resource. In particular, a significant amount (intensity and duration) of surface heating must occur before wind is generated, while consistent wind is required to generate waves. In *fully developed seas*, wind is assumed to have been in steady state for a sufficient duration to generate the maximum wave amplitude attributable to a particular wind velocity. The time integration phenomenon also results in a slowing of the dynamical response to the stimulus. For example, wind velocity slowly diminishes after the solar heating stimulus is removed, while the same is true for wave motion with respect to the wind stimulus.

The distribution of wave energy worldwide is depicted in Figure 1. An interesting characteristic of the wave-energy distribution is that some countries with a relatively high dependence on imported fossil fuels for electricity production (for example, Ireland was at 88% in 2008) have access to significant wave-energy resources (70 kW/m of wave crest). As a case in point, Ireland has the potential to capture 14 TWh of wave energy per year, which is more than half of its annual energy consumption of about 26 TWh. However, a complicating factor is that wave-energy resources are frequently located a significant distance from consumption centers, which is also an issue for other renewable resources [3].

The current poor state of wave-energy technology development is highlighted by the availability of just a few commercially available wave-energy converters (WECs), including the Wave Dragon [5], Pelamis [6], Oyster [7], and Wavestar [8]. The stark contrast in the operational principles of these four devices, as well as the diversity in appearance and operation of the 147 prototypes listed in [9], provides further evidence of the relative immaturity of wave-energy technology. A useful overview of wave-energy devices and technology classification is provided in [10]; see also "Diverse Operating Principles of Wave-Energy Converters."

In addition to the relative lack of progress in basic WEC design, there is, understandably, a corresponding "fertile field" in the development of control system technology to optimize the operation of wave-energy devices. This article will attempt to show that the availability of such control technology is vitally important if WECs are to be serious contenders in the renewable energy arena. Ultimately, energy conversion must be performed as economically as possible to minimize the delivered energy cost, while also maintaining the structural integrity of the device, minimizing wear on WEC components, and operating across a wide range of sea conditions.

Dynamic analysis and control system technology can impact many aspects of WEC design and operation, including device sizing and configuration, maximizing energy extraction from waves, and optimizing energy conversion in the power take-off (PTO) system. Ultimately, commissioned wave-energy devices or "farms" must provide energy at prices competitive with other renewable sources. In the short term, a number of state agencies, including in Portugal and Ireland, have provided guaranteed feed-in tariffs to stimulate the development and proliferation of wave-energy devices, at €0.23/kWh and €0.22/kWh, respectively. As a benchmark for comparison, the cost of domestic electricity in Ireland is currently €0.17/kWh. Some recent analysis suggests that current costs for wave energy are in the region of €1/kWh [11].

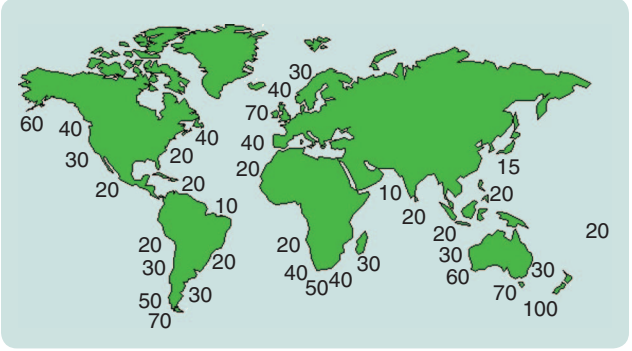

FIGURE 1 An outline global wave map [4]. In general, the latitudes 40–60°, north and south, contain high energy waves. However, proximity to population centers is a major determinant in the utility of wave energy.

Diverse Operating Principles of Wave-Energy Converters

Despite the fact that the earliest wave-energy devices were suggested in the 19th century, the development of wave-energy technology has been slow, and little convergence on an optimum shape, or even operating principle, has been achieved. Figures S1–S3 show a variety of devices, each of which essentially harness wave energy through a different mechanism. However, apart from the device shown in Figure S4, each of the devices harnesses ocean energy through an oscillating motion, and therefore relate directly to the control issues described in this article. Though the device of Figure S4 has natural rectification of wave motion, some interesting control problems are still associated with such devices [S1].

This sidebar is not intended to be a comprehensive overview of the diversity or range of wave-energy devices, nor is the intention to provide a set of classes under which all WECs can be placed. Rather, the intention is to show some of the diversity in operating principles and the lack of convergence in the development of WEC prototypes. For a more comprehensive treatment, the interested reader is referred to [S2] and [S3].

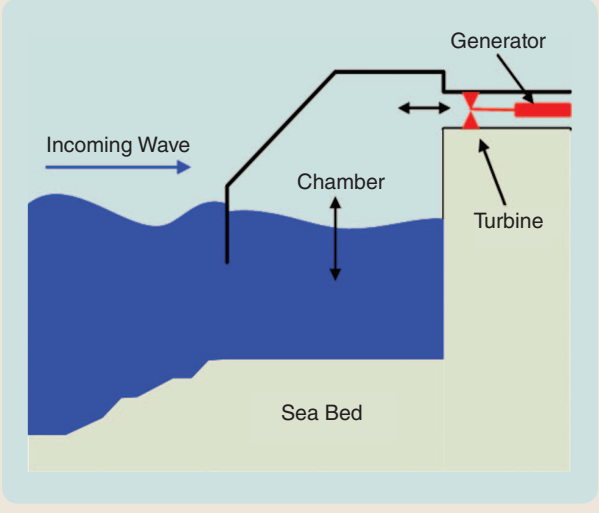

FIGURE S1 A land-based oscillating water column device.

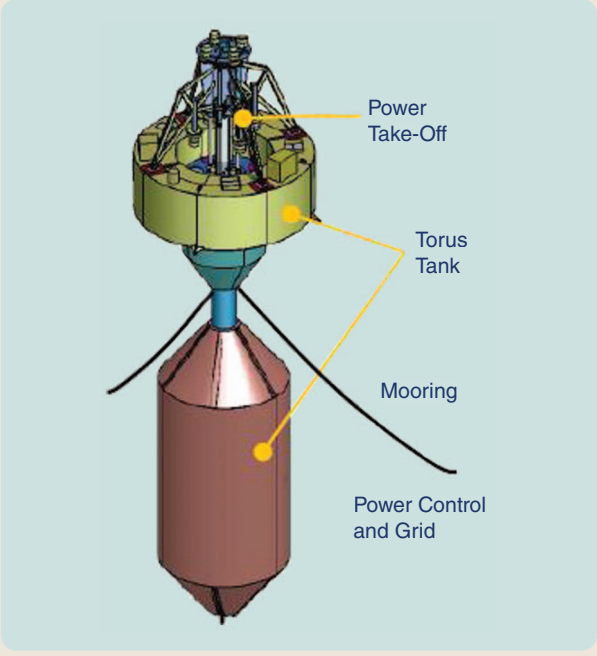

FIGURE S2 The Wavebob device concept is an example of a heaving buoy. Energy is harnessed from the relative motion of the torus and tank.

OSCILLATING WATER COLUMNS

The device shown in Figure S1 is an oscillating water column (OWC), where vertical (heave) motion in the column of water drives air through a turbine. Often, Wells or impulse turbines are used, which provide unidirectional torque to the turbine despite the bidirectional air flow. Both land-based and floating OWC devices have been proposed. Land-based OWCs can be sensitive to tidal height variations.

POINT ABSORBERS

Point absorbers usually harness the heaving motion of the device for conversion to useful energy. Point absorbers have the advantage of being insensitive to wave direction and can be bottom referenced, where motion relative to the seabed is

As a measure of the challenge, since energy density increases by a factor of almost 15 in the conversion from wind to wave, wave devices might be expected to be 15 times smaller than their wind counterparts, for a comparable power output. However, a typical conventional 850-kW horizontal axis wind turbine, such as the Vestas V52–850 kW, has a tower height of 60 m and a rotor diameter of 52 m, whereas the Pelamis WEC rated at 750 kW has a length of 150 m and a diameter of 3.5 m. This rough comparison suggests that considerable improvements to the mechanical design of WECs could still be made. However, since raw renewable resources (such as wind, wave, and tidal) are free, the predominant performance metric [12] for wave energy is the cost of energy delivered to the grid, rather than a pure efficiency measure.

The control community has a significant role to play in making wave-energy extraction economical. While much work remains to be done on optimizing the basic geometry of WECs and the development of efficient PTO systems, it is already clear that appropriate control technology has the capability to double the energy taken from WECs [13]. However, the control problem does not fit neatly into a traditional

captured or can be used to also harness the relative motion between two device components. Figure S2 shows the Wavebob device concept, where the bottom section remains relatively motionless, while the top part (the torus) is sensitive to incident wave motion. The Wavebob device, as shown in Figure S2 employs a hydraulic PTO [S4]. An example of a bottom-referenced point absorber is the Seabased device [S5], which employs a direct electrical PTO.

CONNECTED STRUCTURES

A variety of devices fall into the class of connected structures, including the commercial Pelamis device [S6] and the McCabe wave pump (MWP), shown in Figure S3. Useful power is captured from the relative motion of the device sections. For the Pelamis device, both yaw and pitch motion between sections are accommodated, while the MWP device permits only relative pitch motion.

OVERTOPPING DEVICES

Overtopping devices use a ramp in the incident wave direction to create a forward motion of breaking waves, somewhat like the action of waves on a beach. However, unlike a beach, the forward-progressing waves are captured in a reservoir, which has a mean water height above the mean sea level, as shown in Figure S4. This potential head is then harnessed in a manner similar to a conventional hydroelectric system. Both land-based and floating overtopping devices have been proposed, although land-based schemes can be sensitive to tidal height variations. Ballast control is an important feature of floating overtopping devices [S1].

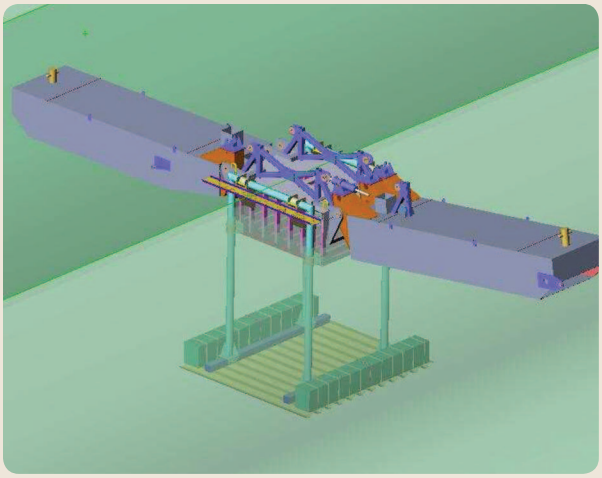

FIGURE S3 The McCabe wave pump harnesses relative pitch motion between sections. An underwater horizontal damper plate is attached to the central section to reduce heave motion.

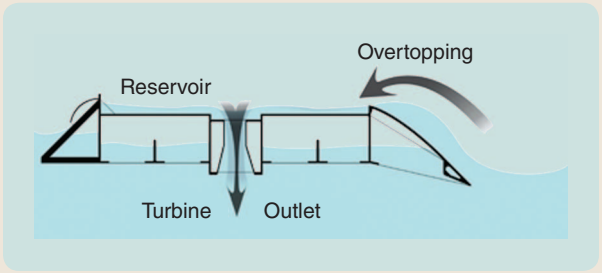

FIGURE S4 Overtopping devices provide natural rectification of the hydraulic power flow and employ a low-head power take-off not dissimilar to conventional hydroelectric systems.

REFERENCES

[S1] J. Tedd, J. Kofoed, M. Jasinski, A. Morris, E. Friis-Madsen, R. Wisniewski, and J. Bendtsen, "Advanced control techniques for WEC wave dragon," in *Proc. 7th European Wave Tidal Energy Conf.*, Porto, Portugal, 2007.

[S2] B. Drew, A. Plummer, and M. Sahinaya, "A review of wave energy converter technology," in *Proc. IMechE Part A: Power and Energy*, 2009, vol. 223, pp. 887–902.

[S3] K. Koca, A. Kortenhaus, H. Oumeraci, B. Zanuttigh, E. Angelelli, M. Cantu, R. Suffredini, and G. Franceschi, "Recent advances in the development of wave energy converters," in *Proc. 9th European Wave Tidal Energy Conf.*, Uppsala, Sweden, 2013.

[S4] K. Schlemmer, F. Fuchshumer, N. Bohmer, R. Costello, and C. Villegas, "Design and control of a hydraulic power take-off for an axi-symmetric heaving point absorber," in *Proc. 9th European Wave Tidal Energy Conf.*, 2011.

[S5] M. Leijon, O. Danielsson, M. Eriksson, K. Thorburn, H. Bernhoff, J. Isberg, J. Sundberg, I. Ivanova, E. Sjöstedt, O. Ågren, K. E. Karlsson, and A. Wolfbrandt, "An electrical approach to wave energy conversion," *Renewable Energy*, vol. 31, no. 9, pp. 1309–1319, 2006.

[S6] R. Yemm, D. Pizer, C. Retzler, and R. Henderson, "Pelamis: Experience from concept to connection," *Philos. Trans. Roy. Soc. A: Math. Phys. Eng. Sci.*, vol. 370, no. 1959, pp. 365–380, 2012.

form such as setpoint tracking, although more traditional regulation loops are required for some special cases such as potable water production [14]. In addition, servo loops are often required in hierarchical WEC control (see the section "Wave-Energy Control Fundamentals").

This article articulates the control problem associated with WECs, examines the structure of a typical WEC model, and provides some examples of how control and associated technologies can be applied to WECs and WEC arrays. An overview of the forecasting problem associated with noncausal control strategies is also given, along with some sample forecasting results, while a comprehensive overview of the general research literature relating to the control of wave-energy devices is contained in the section "Overview of the WEC Control Literature."

QUANTIFYING THE WAVE RESOURCE

The two measurable properties of waves are height and period. Researchers and mariners usually characterize wave heights by the average of the highest one-third of the observed wave heights. This statistically averaged measure is termed the *significant wave height* and usually denoted as $H_{1/3}$ or H_s.

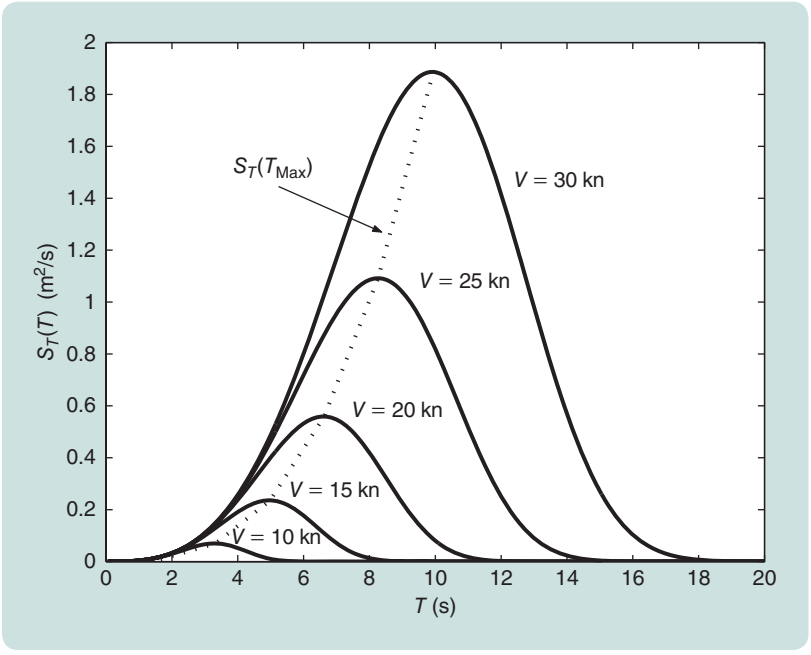

FIGURE 2 A typical Pierson-Moskowitz wave spectra, from (1), for different steady-state wind velocities. Both the wave amplitude and period increase with an increase in the driving wind speed.

In addition, real ocean waves do not generally occur at a single frequency. Rather, a distributed amplitude spectrum is used to model ocean waves, with random phases. Energy spectra are widely used to represent sea states [15]–[18]. The *wave spectral density* (or wave spectrum) has the form

$$S_T(T) = AT^3 e^{-BT^4}, \tag{1}$$

with the coefficients A and B, for example, given for the Pierson-Moskowitz model by [16]

$$A = 8.10 \times 10^{-3} \frac{g^2}{(2\pi)^4}, \tag{2}$$

$$B = 0.74\left(\frac{g}{2\pi V}\right)^4, \tag{3}$$

where V is the wind velocity measured 19.5 m above the still-water level (SWL), g is the acceleration due to gravity, and T is the wave period in seconds. Some typical wave spectra generated from this model are shown in Figure 2. Note that the available wave energy increases (approximately) exponentially with wave period T.

Not all waves are well represented by the spectral models of the type shown in (1). In some cases, where swell and local wind conditions are relatively uncorrelated (which can often be the case, for example, on the west coast of Ireland [19]), "split spectra," consisting of spectra containing two distinct peaks, can occur. The variety of spectral shapes, illustrated in Figure 3, presents a significant challenge to both the WEC designer and control engineer.

All of the aforementioned wave spectral models are for *fully developed waves*; in other words, the fetch (the distance over which the waves develop) and the duration for which the wind blows are sufficient for the waves to achieve their maximum energy for the given wind speed. In addition, linear wave theory is assumed, meaning that waves are well represented by a sinusoidal form, which relies on assuming that there are no energy losses due to friction, turbulence, or other factors and that the wave height H is much smaller than the wavelength λ.

However, not only is the "wind-wave" component in Figure 3 for set G_3 at odds with the spectrum shown in Figure 2, there are three distinct low-frequency components in set G_1. Directional wave analysis [20] can be used

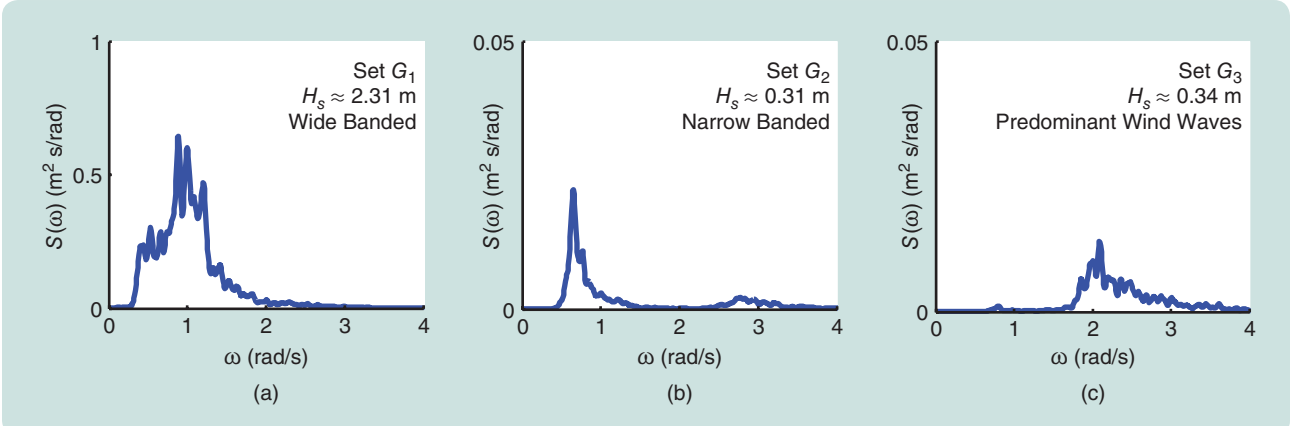

FIGURE 3 Real wave spectra recorded at Galway Bay in Ireland. In general, low-frequency waves have the highest power. Narrow-banded seas make wave forecasting and wave-energy converter control more straightforward, allowing a focus on a predominant single frequency.

to reveal the individual components. In general, with regard to wave directionality, directional wave devices are tethered with nondirectional moorings, which allow the devices to face the predominant wave direction (weather vaning), or devices are nondirectional, such as heaving buoy-type devices.

There are a number of exceptions to this general rule, including shore-mounted oscillating water-column devices, and while many devices can be considered nondirectional, the (fixed) moorings to which they are attached are rarely truly nondirectional.

In general, a wave spectrum is assumed to be stationary for up to 3 h. Time-frequency analysis via the wavelet transform [21] can be used to examine spectral variability. For longer durations, such as a year, wave scatter diagrams (see Figure 4) provide a joint probability table of significant wave heights and characteristic periods for a particular wave site. For example, the data shown in Figure 4 show two predominant wave climates that exist at a particular site.

The energy in an ocean wave, consisting of both potential and kinetic energy, is *proportional to the square of the wave amplitude [2] and proportional to the wavelength*

$$E_w = E_p + E_k = \frac{\rho g H^2 \lambda b}{8}, \tag{4}$$

where H is the wave height above SWL, λ is the wavelength, ρ is the water density, and b is the crest width. In deep water, the energy in a linear wave is equally composed of potential energy (exhibited by the wave height) and kinetic energy (dependent on the motion of the particles)

$$E_p = E_k = \frac{\rho g H^2 \lambda b}{16}. \tag{5}$$

For simulation purposes, wave spectra are usually discretized and individual sinusoidal components used, where the amplitudes are determined from the spectral density (such as in Figure 2), and random initial phases employed for the individual components.

MATHEMATICAL MODELS FOR WAVE-ENERGY DEVICES

Mathematical models of wave-energy devices are required for a variety of purposes:

- assessment of power production
- assessment of loading forces under extreme sea conditions
- simulation of device motion, including evaluating the effectiveness of control strategies
- for use as a basis for model-based control design.

Mathematical models for wave-energy devices should, ideally, encompass the water/device (hydrodynamic) interactions and PTO system and may also include a model for connection to an electrical grid, thus presenting a total "wave-to-wire" model [22]. While the PTO and grid (or possibly other downstream energy consumers, such as reverse osmosis units) may be modeled using more traditional physical lumped-parameter modeling methodologies, the determination of the hydrodynamic model for a WEC, or array of WECs, is nontrivial. A variety of modeling methodologies are available, most of which involve the solution to partial differential equations across a numerical mesh.

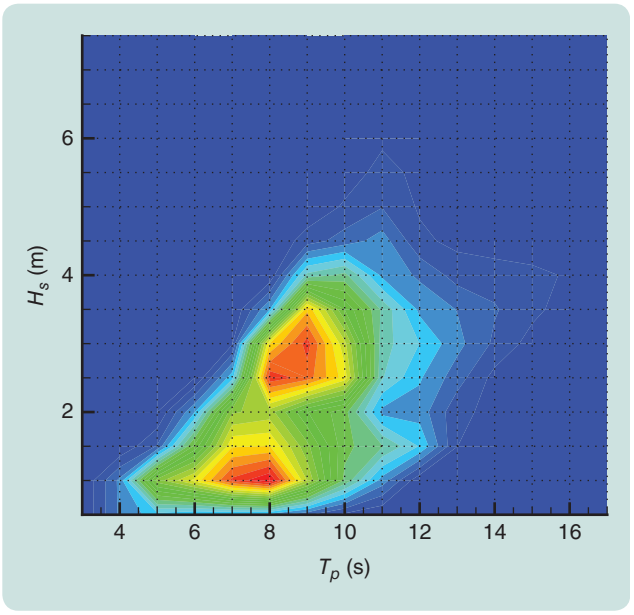

FIGURE 4 A sample scatter diagram for the Atlantic Marine Energy Test Site in Belmullet, Ireland. In general, both peak period, T_p, and significant wave height, H_s, increase together. Typical Atlantic waves cover a period span of 6–12 s.

Among the possible hydrodynamic solvers with the highest fidelity are algorithms based on smooth particle hydrodynamics (SPH) [23] or computational fluid dynamics (CFD) [24]. Such approaches can articulate the full range of nonlinear hydrodynamic forces in three dimensions. However, given the significant computational overhead of such approaches (typically a second of simulation time takes around an hour of computation time), they are not ideal either as a basis for model-based control design nor as a simulation tool to evaluate the effectiveness of various control designs. However, CFD models have been used to develop simpler parametric models, which can provide a basis for control design and simulation [25]. The remainder of this section is primarily devoted to the development of hydrodynamic models. An outline of a possible PTO system is shown in Figure 5 and shows the possible inclusion of mechanical, hydraulic, and electrical components. In many cases, for example, for the SeaBased device [26], the WEC is directly coupled to a linear generator, eliminating the hydraulic components. Given the many potential changes of energy form evident from Figure 5, bond graphs have been shown to be a powerful tool in providing a systematic graphical procedure to determine mathematical

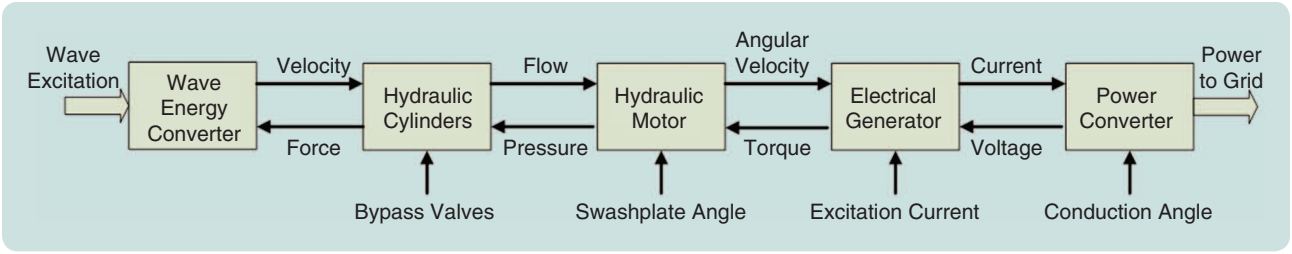

FIGURE 5 Wave-energy power take-off system components and potential control inputs. In general, only one of these control inputs is used by the energy-maximizing control.

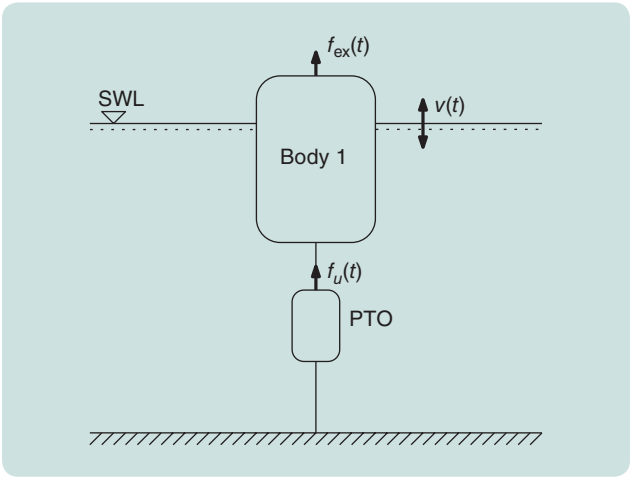

FIGURE 6 A one-degree-of-freedom floating system for wave-energy conversion. The lower side of the power take-off is anchored to the sea bed, which provides an absolute reference for device motion.

models for wave-energy PTO systems [27] or complete wave-energy systems [28].

Linear Models and Cummins' Equation

Consider a single-body floating system oscillating in heave, which is schematically depicted in Figure 6. Energy is extracted from the relative motion with the sea bottom, through a generic PTO mechanism. The external forces acting on the WEC are the excitation from the waves and the control force produced by the PTO, namely $f_{ex}(t)$ and $f_u(t)$. Additional hydrodynamic and hydrostatic forces, which arise due to the motion of the body in the water, are the radiation force $f_r(t)$, the diffraction force $f_d(t)$, the viscous force $f_v(t)$, and the buoyancy force $f_b(t)$ [29].

The radiation force $f_r(t)$ is a damping/inertial force arising due to the fact that device motion, resulting in the production of radiated waves, is affected by the surrounding fluid. Such radiation forces are present even in the absence of incident waves and can be estimated using free response tests. The diffraction (or scattering) force $f_d(t)$ describes the force experienced by the device when scattering incident waves and is independent of the device motion. The viscous damping force $f_v(t)$ is a nonlinear force and becomes significant with increased device velocity. It is particularly relevant where the body surface contains discontinuities (such as flanges), which result in the creation of vortices. Finally, the buoyancy force is related to the deflection of the device from its equilibrium (still water) position and is a balance between the Archimedes buoyancy force and the gravity force.

The equation of motion, following Newton's second law and where a superposition of forces is assumed, in 1 degree-of-freedom (DOF) is

$$M\dot{v}(t) = f_m(t) + f_r(t) + f_d(t) + f_v(t) + f_b(t) + f_{ex}(t) + f_u(t), \tag{6}$$

where $v(t)$ is the heaving velocity and M is the WEC mass.

With the assumptions associated with linear potential theory [29], namely that the fluid is irrotational, incompressible, and inviscid; the WEC body has a small cross-sectional area (or equivalently, the wave elevation is constant across the whole body); and the body experiences small oscillations (so that the wetted surface area is nearly constant); the equation of motion simplifies to

$$f_{ex} + f_d(t) = \int_{-\infty}^{+\infty} h_{ex}(\tau)\eta(t-\tau)d\tau, \tag{7}$$

$$f_r(t) = -\int_0^t h_r(\tau)v(t-\tau)d\tau - m_\infty \dot{v}(t), \tag{8}$$

$$f_b(t) = -\rho g S_w \int_0^t v(\tau)d\tau = -K_b x(t), \tag{9}$$

$$f_v(t) = 0. \tag{10}$$

In (7), the excitation (and diffraction) force is related to the incident wave-free surface elevation $\eta(t)$ through the excitation kernel function $h_{ex}(t)$. Equation (8) expresses the radiation force as a linear convolution of the radiation kernel $h_r(t)$ with the oscillation velocity $v(t)$. Note that $h_{ex}(t)$ and $h_r(t)$ effectively describe the impulse responses in excitation force and radiation force to impulses in free surface elevation and device motion, respectively. Added mass reflects an effective increase in the device inertia since an accelerating floating body moves some volume of the surrounding fluid. In general, added mass is a frequency-dependent quantity but is often approximated by its infinite frequency asymptote m_∞.

The buoyancy force $f_b(t)$ models the hydrostatic equilibrium, related to the heaving position through a linear coefficient that depends on the gravity acceleration g, the water

density ρ, and the surface area of the body cut by the mean water level S_w. Note the noncausality of the expression for the excitation force, where $h_{\text{ex}}(t) \neq 0$ for $t \leq 0$ [29]. Equation (6), excluding the mooring force $f_m(t)$ and the viscous damping force $f_v(t)$, results in the widely used Cummins' equation [30]

$$(M + m_\infty)\dot{v}(t) + \int_0^{+\infty} h_r(\tau)v(t-\tau)d\tau + K_b x(t) = \int_{-\infty}^{t} h_{ex}(\tau)\eta(t-\tau)d\tau. \quad (11)$$

To focus on the control problem, the mooring force $f_m(t)$ is omitted from the following analysis, while the viscous damping force $f_v(t)$ is discussed in the next section. Typically, $h_{\text{ex}}(t)$ and $h_r(t)$ are calculated numerically using boundary-element potential methods such as WAMIT [31], which performs the calculations in the frequency domain, or ACHIL3D [32], where time-domain calculations are used. Equation (11) can also be used to model multibody systems [33] or arrays of devices [34], with the modification that the dimensions of M, m_∞, and K and the hydrodynamic parameters represented by $h_{\text{ex}}(t)$ and $h_r(t)$ all increase in dimension accordingly.

Modeling Higher-Order Hydrodynamic Effects

Linear model (11) assumes sinusoidal waves (or a summation thereof), no viscous effects, and no vortex shedding. In addition, the boundary element methods used to compute $h_{\text{ex}}(t)$ and $h_r(t)$ assume small waves, small device motion (that is, small displacement and velocity), and that the hydrostatic coefficients are constant. While the assumption of small device motion is usually reasonable for systems contained within a regulatory loop (which tries to maintain the system output at a reference point), this assumption is not well satisfied in the case of WECs since it is normally the objective to exaggerate the motion (for example, through resonance) to maximize power capture. Finally, current boundary-element solvers typically use a fixed mesh, although some new approaches are now appearing that use adaptive meshes [35]. However, the computational effort increases considerably with adaptive meshing.

Ideally, nonlinear device motion and nonlinear interactions between the incident wave field and the diffraction and radiation potentials should be considered, potentially resulting in coupling between different motions and generating parametric resonance effects [36]. Possible device submergence can be taken into account using potential methods, which cannot take into account wave breaking effects since their effects are calculated only from a "potential" point of view.

Numerical methods for partial or fully nonlinear hydrodynamic modeling have been developed [37], and several commercial software packages are already on the market such as FREDYN [38] and LAMP [39]. Among these latter methods, a possible extension of the linear time-domain model is to compute the nonlinear Froude-Krylov forces on the undisturbed wetted surface, while diffraction-radiation forces remain linear or are expanded up to the second-order [40], [41]. Hence, the hydrodynamic force τ_H may be decomposed into six terms as

$$\tau_H = \tau_B + \tau_{\text{FK}} + \tau_{\text{Rad}}^{(1)} + \tau_{\text{Diff}}^{(1)} + \tau_{\text{Rad}}^{(2)} + \tau_{\text{Diff}}^{(2)}, \quad (12)$$

where indexes (1) and (2) denote the first- and second-order solutions for both diffraction and radiation force. For example, [42] calculates Froude-Krylov forces both on the instantaneous and exact wetted surfaces to compare the power production for linear and nonlinear WEC models. The assumption is that the Froude-Krylov forces are large compared to diffraction and radiation forces, which are modeled using linear terms. The study in [42] clearly shows that linear models *overestimate* WEC motion for large wave excitation. A slightly alternative formulation is presented in [43]. The difficulty of employing such approaches is the need for recalculation of hydrodynamic parameters at each simulation step, which renders such methods computationally inappropriate as a basis for model-based control, although the methods could possibly be used for high-fidelity simulation.

If desired, nonlinear viscous forces can be added [for example, to (11)] using a term experimentally derived by [44], such as

$$f_v(t) = \rho R C_d |v(t)| v(t) \quad (13)$$

for a cylindrical shape, where ρ is the water density, R is the cylinder radius, and C_d is the drag coefficient. Empirical validations of (13) have proven its validity, and methods have been proposed to evaluate the coefficient C_d for certain specific shapes [45], [46]. In addition, a linear approximation to (13) may be derived, using an energy-matching technique [47] if desired.

In addition, nonlinear PTO effects, such as saturation, nonideal efficiency, and other static nonlinearities, could be considered but are beyond the scope of this review, given the wide variety of PTO system components available.

Figure 7 considers nonlinear effects within the context of overall WEC operation. As the motion becomes more

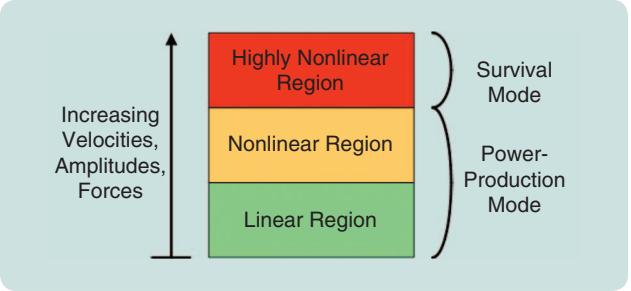

FIGURE 7 Wave-energy converter (WEC) operational modes and nonlinear behavior. Most WECs need to enter a survival mode in extreme wave conditions to avoid structural damage.

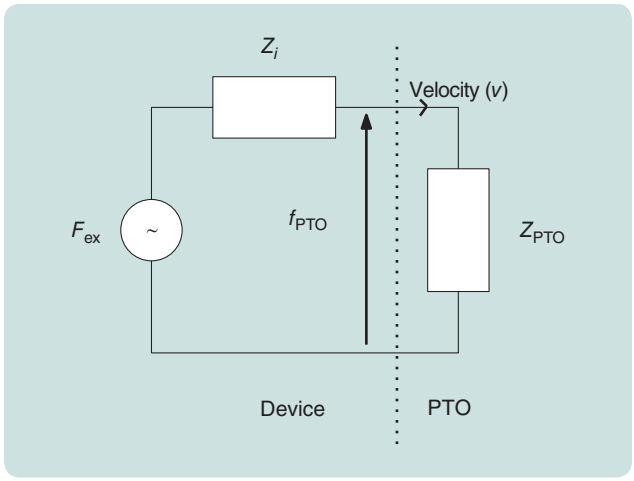

FIGURE 8 Impedance matching for a wave-energy device, directly analogous to its electric circuit counterpart.

exaggerated, nonlinear effects become more predominant. However, from a control perspective, nonlinearity is only an issue within the power production mode. Beyond a "safe" operating region, supervisory control is normally used to put the device into survival mode, which limits motion and allows extreme wave forces to be tolerated while maintaining device integrity.

Radiation Damping Approximations

Typically, for both simulation and control applications, the radiation damping convolution term in (8) is replaced by a closed-form (finite-order) equivalent. This replacement has several advantages. The integrodifferential equation in (11) is replaced by a higher-order differential equation, making analysis more straightforward, the resulting finite-order dynamical system is faster to simulate, and the closed-form dynamical equation can be used as a basis for model-based control design.

In general, $h_r(t)$ (and its Fourier transform, $H_r(\omega)$) are nonparametric in form, being the result of a numerical calculation on a distributed system. Approximations can be determined in either the time or frequency domain, depending on the manner in which $h_r(t) \leftrightarrow H_r(\omega)$ was determined and the intended (time/frequency domain) use of the finite-order approximation. For example, WAMIT [31] uses a frequency-domain analysis to determine $H_r(\omega)$ directly and approximations based on WAMIT data are usually based on frequency-domain error criteria. In such a case, state-space forms [48] or transfer function forms [49] may be determined using frequency-domain identification [50].

Alternatively, if $h_r(t)$ is directly produced, for example from the time-domain code ACHIL3D [32], time-domain impulse-response fitting can be employed, typically using the method in [51]. In general, an order 4–10 linear approximation to $h_r(t)$ is used, for both time- and frequency-domain approaches. In some cases, a second-order approximation is adequate and has the added advantage of giving a pole pair, which has a strong connection with the radiation damping transient response. Reference [52] provides an overview of, and background on, the calculations of finite-order approximations to $h_r(t) \leftrightarrow H_r(\omega)$. Reference [52] also considers finite-order approximation to the excitation force kernel $h_{ex}(t)$ (with Fourier transform $F_{ex}(\omega)$) as does [49].

WAVE-ENERGY CONTROL FUNDAMENTALS

To consider the control problem for wave-energy devices, define the control objective

```
Maximize      Performance objective (maxi-
              mize energy)
subject to:   Constraints (amplitudes, forc-
              es, etc.)
```

Ignoring system constraints for the moment, a start can be made on the energy maximization problem by considering the force-to-velocity model of a WEC, which is obtained from (11) in the frequency domain [29] as

$$\frac{V(\omega)}{F_{ex}(\omega) + F_u(\omega)} = \frac{1}{Z_i(\omega)}, \tag{14}$$

where $Z_i(\omega)$ is termed the *intrinsic impedance* of the system. In (14), $V(\omega)$, $F_{ex}(\omega)$, and $F_u(\omega)$ represent the Fourier transform of the velocity $v(t)$, excitation force $f_{ex}(t)$, and control force $f_{PTO}(t)$, respectively. Unless stated otherwise, the Fourier transform of time-domain signals or functions will be denoted by the corresponding capital letter, namely $X(\omega) \triangleq \mathcal{F}\{x(t)\}$.

The intrinsic impedance $Z_i(\omega)$ of the model in (14) is specified as (see [29] for the full derivation)

$$Z_i(\omega) = B_r(\omega) + \jmath\omega\left[M + M_a(\omega) - \frac{K_b}{\omega^2}\right], \tag{15}$$

where $B_r(\omega)$ is the radiation resistance (real and even) and $M_a(\omega)$ is the frequency-dependent added mass, often replaced by its high-frequency asymptote m_∞.

The model in (14) allows the derivation of conditions for optimal energy absorption and the intuitive design of the energy-maximizing controller in the frequency domain [29] as

$$Z_{PTO}(\omega) = Z_i^*(\omega), \tag{16}$$

where $(\,)^*$ denotes the complex conjugate. The choice of Z_{PTO} as in (16) is referred to as *complex conjugate control*, but many (especially electrical) engineers will recognize this choice of Z_{PTO} as the solution to the impedance-matching problem represented by Figure 8. The result in (16) has a number of important implications.

- The result is frequency dependent, implying that there is a different optimal impedance for each frequency, which raises the question of how to specify the PTO resistance for irregular seas containing a mixture of frequencies.

» Since $h_r(t)$ is causal, $h_c(t) = \mathcal{F}^{-1}(Z_{\text{PTO}}(\omega))$ is anticausal, requiring future knowledge of the excitation force. While this knowledge is straightforward for the monochromatic case (single sinusoid), it is more problematic for irregular seas. The issue of forecasting random seas is dealt with in the section "Wave Forecasting."

» Since force and velocity can have opposite signs in Figure 8, the PTO may need to *supply* power for some parts of the sinusoidal cycle, which is akin to reactive power in electrical power systems. Such a phenomenon places particular demands on PTO systems, not only in terms of the need to facilitate bidirectional power flow but also that the peak reactive power can be significantly greater than active power [53], [54]. The optimal *passive* PTO is provided by $R_{\text{PTO}} = |Z_i(\omega)|$, which avoids the need for the PTO to supply power but results in a suboptimal control.

» The optimal control in (16) takes no account of physical constraints in the WEC/PTO, where there are likely to be limitations on displacement or relative displacement, and the PTO force, and there may be external constraints imposed by electrical grid regulations.

The condition in (16) can alternatively be expressed in terms of an optimal velocity profile as

$$V^{\text{opt}}(\omega) = F_{\text{ex}}(\omega) / (2R_i(\omega)), \tag{17}$$

where $R_i = 1/2(Z_i + Z_i^*)$ is the real part of Z_i. The condition in (17) is a condition on the amplitude of $V^{\text{opt}}(\omega)$, with the restriction that $v^{\text{opt}}(t)$ be in phase with $f_{\text{ex}}(t)$, since R_i is a real (and even) function. This phase condition, considered separately, forms the basis for some simple WEC *phase control* strategies, such as *latching*. See "Discrete Control—Latching and Declutching" for further details.

While the conditions of (16) and (17) specify the optimal device velocity profile, the conditions do not specify how the velocity profile might be achieved. Figure 9 shows a hierarchical structure for WEC control, where the optimal velocity is calculated in the upper branch and the PTO force is used to achieve this velocity in the lower servo loop. Figure 9 highlights the calculation of the optimal velocity profile as an open-loop calculation, which is therefore sensitive to modeling errors. Robustness must be addressed, which is considered in the section "Simple but Effective Control." The control structure of Figure 9 is also used by most wind turbine controllers, where the optimum power coefficient C_p is determined from blade pitch angle β and tip speed ratio λ, and generator torque control is then typically used to achieve the tip speed ratio that maximizes C_p, where $C_p = f_{\text{turbine}}(\beta, \lambda)$ [55].

Control Effectors

Since wave-energy PTO systems typically involve a number of changes of energy form, there can be a variety of ways to implement the required f_{PTO} to achieve the desired device velocity. Figure 5 shows a number of possible variables that can be manipulated to control the PTO force, which opposes the WEC device motion, including the hydraulic motor swash-plate angle, the generator excitation current, and the power converter conduction angle.

In general, only one of these inputs is used, although consideration of efficiency of the various PTO components suggests that some combination may be beneficial. An additional input, for WECs where multiple hydraulic cylinders or (linear) electrical generators are used, could be the number of cylinders/generators employed either on a wave-to-wave basis or for significant changes in sea state. Hydraulic bypass valves could be used to deactivate hydraulic cylinders, while linear generators could be electrically short-circuited. A final control possibility is that of a pumpable water ballast, which can be used to alter the WEC inertia and therefore change its resonant frequency [which is predominantly related to M and K_b in (11)]. An example study using ballast control for a bottom-hinged flap was performed by [56]. However, the use of water ballast as a control input has limitations, including maximum pumping rate (determined by pump size) and the energy cost of moving water ballast is also an important consideration.

REAL-TIME CONTROL OF WAVE-ENERGY CONVERTERS

This section details two possibilities for real-time control of WECs, both of which handle system constraints. The methods are at opposite ends of the complexity/performance spectrum and so provide reasonable indicators of the range of WEC control algorithms available. In addition, a comprehensive literature overview of WEC control algorithms is provided in the section "Overview of the WEC Control Literature."

Simple but Effective Control

Consider (17), which calculates the optimal velocity profile as a (frequency-dependent) function of the excitation force for the system as shown in Figure 6. Below, a suboptimal approximation of reactive control is proposed, where the

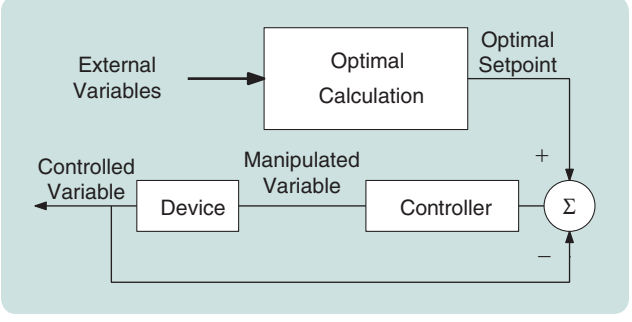

FIGURE 9 A hierarchical control structure, showing the optimal setpoint (feedforward) calculation and the servomechanism section that adjusts the power take-off so that the optimal (force/velocity) setpoint is achieved.

Discrete Control—Latching and Declutching

Latching and declutching belong to the class of *discrete control algorithms*, that is, algorithms that implement an on/off PTO force, usually through a braking mechanism (latching) or PTO bypass (declutching). Latching and declutching can be combined, in which case the conversion performance increases considerably compared to latching or declutching individually [S7]. Figure S5 shows the principle of operation of both schemes. The red arrows show the position and operational mode of the latch or clutch. For simplicity, the PTO is assumed to implement linear damping (that is, $f_{\mathrm{PTO}}(t) = B_{\mathrm{PTO}} v(t)$, where v is the device velocity) and the excitation is assumed to monochromatic, that is, a single sinusoid.

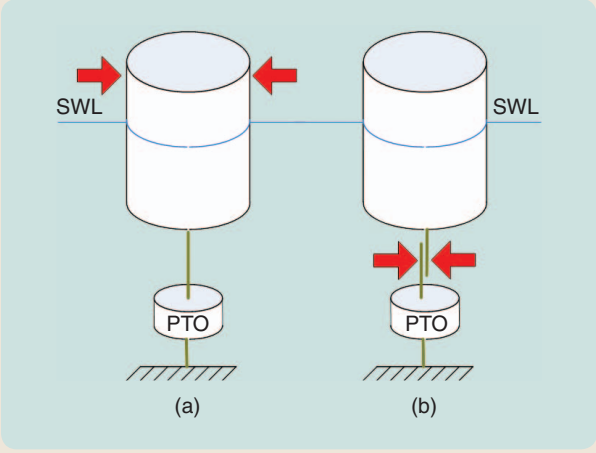

FIGURE S5 Discrete control principles of operation. On/off power take-off (PTO) control can be implemented either through a braking mechanism, called (a) latching, or by bypass, called (b) declutching.

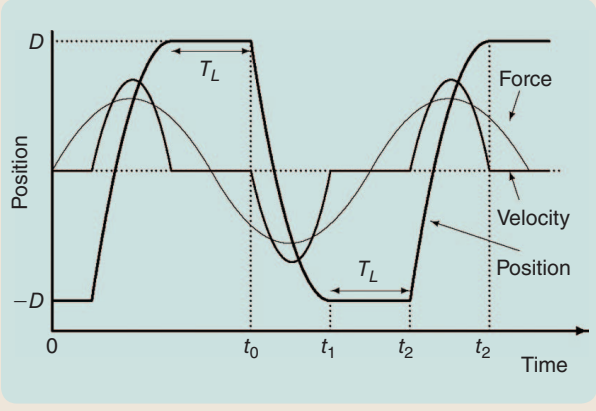

FIGURE S6 The evolution of system variables under latching control.

LATCHING

In latching, the device motion is locked at various points in the wave cycle, particularly at the extrema of displacement, where the device velocity is zero. As a result, the braking effect is similar to a car handbrake, where the brake is applied at zero velocity and reliance is made on static friction to prevent motion. Figure S6 shows how the system variables evolve under a latching strategy. Latching is applied at time t_1 and the device is released at t_2 after a latched duration T_L, and similarly for positive displacements, effectively increasing the potential energy during each half cycle. Though the velocity is zero for parts of the cycle, the overall energy capture is increased, since the velocity, while quite nonlinear, is "in phase" with the excitation force.

In the late 1970s, several researchers independently proposed latching [S8]–[S10], which satisfies the optimal phase condition only [S11], that is, the WEC device is in phase with force. Though most suitable only for incident waves with periods larger than the resonant period of the oscillating body, [S12] showed that latching has better energy absorption, compared to a linear PTO damping, when the period of the incident wave is shorter than the resonance period of the device. For polychromatic waves, the concept of phase between excitation force and velocity is not well defined, in which case the objective of optimization of the latching interval is not unique [S12]. In this case, the latching time can be optimized to synchronize the peak of the velocity with the peak of the excitation force [S13] or to maximize the absorbed power [S14].

Latching control fundamentals are presented in [S15]–[S17]. Latching and some of its variants have been extensively analyzed from both the theoretical and practical points of view in [S18]. Detailed modeling and comprehensive simulation results from the application of latching control to a heaving hemisphere and to two vertical cylinders are given in [S19] and for a heaving hemisphere in [S20]. In [S21], latching control is implemented using neural networks, while [S22] studies the effects on the grid of the power produced by a WEC controlled with latching.

A control algorithm that exploits the natural Coulomb damping characteristic of a hydraulic PTO to implement latching was designed in [S23]. The same approach was taken with a two-body device in [S24], where the improvement in converted energy provided by latching was shown to be not as significant as for the single-body case. Latching control was also tested on a two-body device with a hydraulic PTO, which reached similar conclusions [S25]. More recent studies [S26], [S27], however, found that latching control applied to a two-body device can increase the annual average power output by up to five times.

Simulations of latching control have been used to compare the absorbed power of a two-body WEC to an equivalent single-body system connected to the seabed [S28], [S29]. Simulation of a two-body, force-compensated WEC subject to latching control is provided in [S30]. In [S31], latching control is applied to the Wavebob device with a hydraulic PTO.

Experimental applications of latching on prototypes have been reported in [S32]–[S35]. Latching control has also been tested in many experimental prototypes, including on the Buldra [S36], the first prototype of the AWS [S37]–[S39], and the SEAREV device [S14], [S40]–[S42].

Analytical computation of the optimal latching duration for monochromatic waves is reported in [S43], while numerical optimization is used to derive the optimal latching duration in [S28] and [S29] for random and monochromatic seas. Several latching control strategies in regular and random seas have been compared using a semianalytic solution for the latching period [S12], [S14]. A similar approach was taken in [S44], and a sensitivity analysis of the power converted using latching control for the SEAREV device is described in [S45].

The phase control of a heaving-buoy WEC subject to amplitude constraints is described in [S46]–[S48]. The applied phase control, which aims to keep the velocity in phase with the excitation force, produces results similar to latching. The optimality of latching, in terms of a nonlinear PTO force profile over the wave period, was shown in [S49]. As an extension to this study, a broader set of sea periods was examined in [S50], which showed that latching is only optimal when the dominant sea period is slower than the device resonant period.

DECLUTCHING

In declutching, the device is unloaded at specific points in the cycle, as indicated by the intervals marked in Figure S7. Declutching, also called *freewheeling* or *unlatching*, was considered originally in [S51]. Subsequently, declutching was applied to the SEAREV device to obviate a characteristic effect of hydraulic PTOs known as Coulomb damping [S52], [S53].

Declutching has also been studied in [S50], which shows that declutching is an optimal nonlinear damping strategy when the device resonant period is longer than the sea period. Effectively, unloading the device during the declutching periods allows the device to "catch up" to the excitation force, which brings the device velocity (though nonlinear) into phase with the excitation force.

A substantial increase in energy absorption compared to latching or declutching implemented independently has been shown recently [S7]. Active bipolar damping control, which is a combination of latching and declutching, has been simulated and implemented [S54].

OPTIMALITY OF LATCHING AND DECLUTCHING

While neither declutching nor latching implement optimal complex conjugate control, they offer potentially simple (no need for reactive power flow) methods to achieve resonance when the device resonant period is longer (declutching) or shorter (latching) than the wave period. Achieving resonance has the effect of broadening the response amplitude operator (frequency response) of the device, as shown in Figure S8.

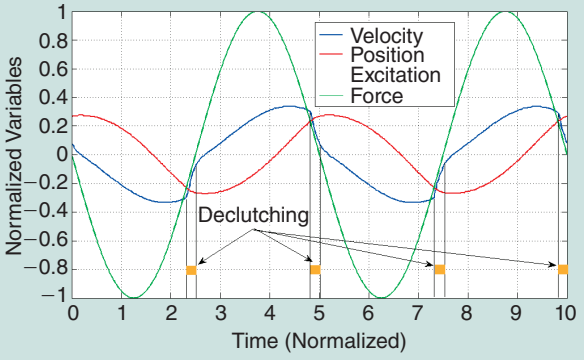

FIGURE S7 The evolution of system variables under declutching control.

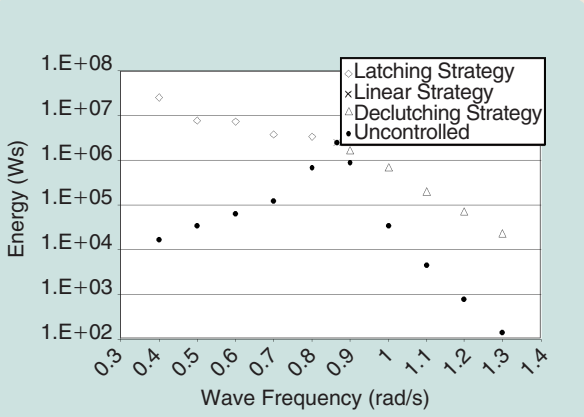

FIGURE S8 The modification of the device response amplitude operator under latching and declutching.

Other nonlinear damping protocols, over each wave period, can be considered. However, it has been shown [S50] that, in general, for monochromatic seas and linear system models, latching (declutching) is optimal when the device resonant period is shorter (longer) than the wave period.

REFERENCES

[S7] A. H. Clement and A. Babarit, "Discrete control of resonant wave energy devices," *Philos. Trans. Roy. Soc. A, Math. Phys. Eng. Sci.*, vol. 370, no. 1959, pp. 288–314, 2012.

[S8] K. Budal and J. Falnes, "A resonant point absorber of ocean wave power," *Nature*, vol. 256, pp. 478–479, Aug. 1975.

[S9] D. Guenther, D. Jones, and D. Brown, "An investigative study of a wave-energy device," in *Proc. Midwest Energy Conf.*, Chicago, IL, Nov. 1979, vol. 4, pp. 299–306.

[S10] M. J. French, "A generalized view of resonant energy transfer," *J. Mech. Eng. Sci.*, vol. 21, no. 4, pp. 299–300, 1979.

[S11] J. Falnes, "Optimum control of oscillation of wave-energy converters," in "Annex Report B1: Device Fundamentals/Hydrodynamics of the Wave Energy Converters: Generic Technical Evaluation Study," Inst. Fysikk, Norwegian University of Science and Technology, Trondheim, Norway, Contract JOU2-0003-DK, Tech. Rep., Aug. 1993.

[S12] A. Babarit, G. Duclos, and A. Clement, "Comparison of latching control strategies for a heaving wave energy device in random sea," *Appl. Ocean Res.*, vol. 26, no. 5, pp. 227–238, 2004.
[S13] J. Hals, T. Bjarte-Larsson, and J. Falnes, "Optimum reactive control and control by latching of a wave-absorbing semisubmerged heaving sphere," in *Proc. ASME Conf.*, 2002, pp. 415–423.
[S14] A. Babarit and A. Clement, "Optimal latching control of a wave energy device in regular and irregular waves," *Appl. Ocean Res.*, vol. 28, no. 2, pp. 77–91, 2006.
[S15] J. Falnes, "Principles for capture of energy from ocean waves. Phase control and optimum oscillation," Dept. Phys., NTNU, Trondheim, Norway, Tech. Rep. N-7034, 1997.
[S16] J. Falnes, *Ocean Waves and Oscillating Systems*. Cambridge, U.K.: Cambridge Univ. Press, 2002.
[S17] J. Falnes, "A review of wave-energy extraction," *Marine Struct.*, vol. 20, no. 4, pp. 185–201, Oct. 2007.
[S18] J. A. M. Cretel, A. Lewis, G. Thomas, and G. Lightbody, "A critical assessment of latching as control strategy for wave-energy point absorbers," in *Proc. 21st Int. Offshore Polar Engineering Conf.*, 2011, pp. 680–686.
[S19] M. Greenhow and S. P. White, "Optimal heave motion of some axisymmetric wave energy devices in sinusoidal waves," *Appl. Ocean Res.*, vol. 19, nos. 3–4, pp. 141–159, 1997.
[S20] F. Kara, "Time domain prediction of power absorption from ocean waves with latching control," *Renew. Energy*, vol. 35, no. 2, pp. 423–434, 2010.
[S21] T. Mundon, A. Murray, J. Hallam, and L. Patel, "Causal neural control of a latching ocean wave point absorber," in *Artificial Neural Networks: Formal Models and Their Applications (ICANN)*. Berlin Heidelberg, Germany: Springer, 2005, pp. 423–429.
[S22] M. Molinas, O. Skjervheim, P. Andreasen, T. Undeland, J. Hals, T. Moan, and B. Sorby, "Power electronics as grid interface for actively controlled wave energy converters," in *Proc. Int. Conf. Clean Electrical Power*, O. Skjervheim, Ed., 2007, pp. 188–195.
[S23] A. F. de O. Falcão, "Phase control through load control of oscillatingbody wave energy converters with hydraulic PTO system," *Ocean Eng.*, vol. 35, nos. 3–4, pp. 358–366, 2008.
[S24] A. F. d. O. Falcão, P. A. P. Justino, J. C. C. Henriques, and J. M. C. S. André, "Reactive versus latching phase control of a two-body heaving wave energy converter," in *Proc. European Control Conf.*, 2009.
[S25] J. J. Candido and P. A. Justino, "Modelling, control and Pontryagin maximum principle for a two-body wave energy device," *Renew. Energy*, vol. 36, no. 5, pp. 1545–1557, 2011.
[S26] J. C. C. Henriques, M. F. P. Lopes, R. P. F. Gomes, L. L. M. Gato, and A. F. de O. Falcao, "Performance evaluation of a two-body heaving WEC with latching control using a new numerical method," in *Proc. 9th European Wave Tidal Energy Conf.*, Southampton, 2011.
[S27] J. Henriques, M. Lopes, R. Gomes, L. Gato, and A. Falcao, "On the annual wave energy absorption by two-body heaving WECS with latching control," *Renew. Energy*, vol. 45, pp. 31–40, Sept. 2012.
[S28] U. A. Korde, "Phase control of floating bodies from an on-board reference," *Appl. Ocean Res.*, vol. 23, no. 5, pp. 251–262, 2001.
[S29] U. Korde, "Latching control of deep water wave energy devices using an active reference," *Ocean Eng.*, vol. 29, no. 11, pp. 1343–1355, 2002.
[S30] J. Hals, R. Taghipour, and T. Moan, "Dynamics of a force-compensated two-body wave energy converter in heave with hydraulic power takeoff subject to phase control," in *Proc. 7th European Wave Tidal Energy Conf.*, Porto, Portugal, Sept. 2007.
[S31] K. Schlemmer, F. Fuchshumer, N. Bohmer, R. Costello, and C. Villegas, "Design and control of a hydraulic power take-off for an axisymmetric heaving point absorber," in *Proc. 9th European Wave Tidal Energy Conf.*, Southampton, 2011.
[S32] T. Bjarte-Larsson and J. Falnes, "Investigation of phase-controlled wave-power buoy," in *Proc. 6th European Wave Tidal Energy Conf.*, Glasgow, 2005, pp. 47–50.
[S33] J. Falnes and T. Bjarte-Larsson, "Theoretical and experimental investigation of wave energy conversion by a phase-controlled heaving body," *Proc. Inst. Mech. Eng. M*, vol. 220, no. 4, pp. 175–183, 2006.
[S34] T. Bjarte-Larsson and J. Falnes, "Laboratory experiment on heaving body with hydraulic power take-off and latching control," *Ocean Eng.*, vol. 33, no. 7, pp. 847–877, 2006.

noncausality and constraints are handled in a simple, but effective, way. The essence of this algorithm is the assumption that $f_{\text{ex}}(t)$ is a narrow-banded harmonic process, defined by time-varying amplitude $A(t)$, frequency $\omega(t)$, and phase $\varphi(t)$ as

$$f_{\text{ex}}(t) = A(t)\cos(\omega(t)t + \varphi(t)). \tag{18}$$

The optimal reference velocity can then be generated from the adaptive law

$$v_{\text{ref}}(t) = \frac{1}{H(t)} f_{\text{ex}}(t), \quad \frac{1}{H(t)} = \frac{1}{2R_i(\hat{\omega})}, \tag{19}$$

where the value of the constant $H(t)$ is calculated from the curve $1/2B(\omega)$, based on a real-time estimate of the peak frequency of the wave excitation force. An online estimate of the frequency $\hat{\omega}$ and amplitude $\hat{A}$ is obtained via the extended Kalman filter (EKF) [57]. Based on the narrow-banded assumption of (18), the excitation force can be expressed in complex notation as

$$f_{\text{ex}}(t) = \Re\{Ae^{\jmath\varphi}e^{\jmath\omega t}\}, \quad \hat{F}_{\text{ex}} \triangleq Ae^{\jmath\varphi}, \tag{20}$$

where $\hat{F}_{\text{ex}}$ is the complex amplitude of $f_{\text{ex}}(t)$.

As a consequence of the proportional reference-generation law in (19), the complex amplitude of the velocity $\hat{V}$ and position $\hat{U}$ can be expressed as

$$\hat{V} = \frac{A}{H}e^{\jmath\varphi} \tag{21}$$

$$\hat{U} = \frac{\hat{V}}{\jmath\omega} = \frac{A}{\jmath\omega H}e^{\jmath\varphi}. \tag{22}$$

Suppose that the vertical excursion of the WEC is limited to $\pm U_{\text{lim}}$ m from equilibrium. From (22), the position constraint can be written as an equivalent velocity constraint

$$\hat{U} = \frac{\hat{V}}{\jmath\omega} \le U_{\text{lim}} \Leftrightarrow |\hat{V}| \le \omega U_{\text{lim}} \tag{23}$$

and an upper bound for the variable gain, $1/H$, involving the amplitude and frequency of the excitation, can be derived from (21) as

$$\frac{1}{H} \le \frac{\omega U_{\text{lim}}}{A}. \tag{24}$$

The reference generation strategy, based on (17), (19), and (24), can therefore be modulated to keep the amplitude of the velocity within the bound specified in (23). A real-time estimate of the frequency $\hat{\omega}$ and amplitude $\hat{A}$ of the excitation

[S35] J. Falnes and P. Lillebekken, "Budal's latching-controlled-buoy type wave-power plant," in *Proc. 5th European Wave Energy Conf.*, Cork, Ireland, 2003, pp. 233–244.
[S36] H. Lendenmann, K.-C. Stromsem, M. Dai Pre, W. Arshad, A. Leirbukt, G. Tjensvoll, and G. T., "Direct generation wave energy converters for optimized electrical power production," in *Proc. 7th European Wave Tidal Energy Conf.,* Porto, Portugal, 2007.
[S37] P. Beirão, D. Valério, and J. S. da Costa, "Phase control by latching applied to the Archimedes wave swing," in *Proc. 7th Portuguese Conf. Automatic Control*, Porto, Portugal, 2006.
[S38] D. Valério, P. Beirão, and J. S. da Costa, "Optimisation of wave energy extraction with the Archimedes wave swing," *Ocean Eng.*, vol. 34, nos. 17–18, pp. 2330–2344, 2007.
[S39] D. Valério, P. Beirão, M. J. G. C. Mendes, and J. S. da Costa, "Robustness assessment of model-based control for the Archimedes wave swing," in *Proc. European Control Conf.*, Uppsala, Sweden, 2009.
[S40] A. Babarit and A. H. Clément, "Optimal latching control of a wave energy converter," in *Proc. 6th European Wave Tidal Energy Conf.*, Glasgow, 2005, pp. 19–26.
[S41] M. Durand, A. Babarit, B. Pettinotti, O. Quillard, J. Toularastel, and A. Clément, "Experimental validation of the performances of the SEAREV wave energy converter with real time latching control," in *Proc. 7th European Wave Tidal Energy Conf.*, Porto, Portugal, 2007.
[S42] M. Kamensky, M. Guglielmi, and A. Formal'skii, "Optimal switching control of an absorber ocean wave energy device," in *Proc. 2008 16th Mediterranean Conf. Control Automation*, 2008, pp. 785–790.
[S43] A. Babarit, G. Duclos, A. Clément, and J. Gilloteaux, "Latching control of a power take off oscillator carried by a wave activated body," in *Proc. Int. Workshop Water Waves Floating Bodies*, Longyearbyen, Norway, 2005.
[S44] G. Nolan, J. Ringwood, W. Leithead, and S. Butler, "Optimal damping profiles for a heaving buoy wave-energy converter," in *Proc. 15th Int. Offshore Polar Engineering Conf.*, Seoul, Korea, 2005.
[S45] A. Babarit and A. Clement, "Application of the optimal command method to the control of the SEAREV wave energy converter: A study on the influence of time constants on the efficiency of the latching control," in *Proc. 10th European Control Conf.*, Budapest, Hungary, 2009, pp. 245–257.
[S46] H. Eidsmoen, "Simulation of a tight-moored amplitude limited heaving-buoy wave-energy converter with phase control," Division Phys., Norwegian Univ. Sci. Technol., NTNU, Trondheim, Norway, Tech. Rep., 1996.
[S47] H. Eidsmoen, "Simulation of a slack-moored heaving-buoy wave-energy converter with phase control," Division Phys., Norwegian Univ. Sci. Technol., NTNU, Trondheim, Norway, Tech. Rep., May 1996.
[S48] H. Eidsmoen, "Tight-moored amplitude-limited heaving-buoy wave-energy converter with phase control," *Appl. Ocean Res.*, vol. 20, no. 3, pp. 157–161, 1998.
[S49] J. Ringwood and S. Butler, "Optimisation of a wave energy converter," in *Proc. IFAC Conf. Control Application Marine Systems,* Ancona, Italy, 2004, pp. 155–160.
[S50] B. Teillant, J.-C. Gilloteaux, and J. Ringwood, "Optimal damping profile for a heaving buoy wave energy converter," in *Proc. IFAC Conf. Control Applications Marine Systems*, 2010, pp. 393–398.
[S51] A. Wright, W. Beattie, A. Thompson, S. Mavrakos, G. Lemonis, K. Nielsen, B. Holmes, and A. Stasinopoulos, "Performance considerations in a power take-off unit based on a non-linear load," in *Proc. 5th European Wave Energy Conf.*, Cork, Ireland, 2003.
[S52] A. Babarit, M. Guglielmi, and A. H. Clement, "Declutching control of a wave energy converter," *Ocean Eng.*, vol. 36, nos. 12–13, pp. 1015–1024, 2009.
[S53] A. Babarit, H. Mouslim, M. Guglielmi, and C. A. H., "Simulation of the SEAREV wave energy converter with a by-pass control of its hydraulic power-take-off," in *Proc. World Renewable Energy Congr.*, Glasgow, U.K., 2008.
[S54] M. Folley and T. Whittaker, "The control of wave energy converters using active bipolar damping," in *Proc. Inst. Mech. Eng. M, J. Eng. Maritime Environ.*, vol. 223, no. 4, pp. 479–487, 2009.

can be obtained through the EKF [58], [59] and the feedforward gain $1/H(t)$ adjusted according to

$$\frac{1}{H(t)} = \begin{cases} \dfrac{1}{2R_i(\hat{\omega})}, & \text{if } \dfrac{\hat{\omega}U_{\lim}}{\hat{A}} > \dfrac{1}{2R_i(\hat{\omega})} \\ \dfrac{\omega U_{\lim}}{\hat{A}}, & \text{otherwise} \end{cases} \tag{25}$$

According to (25), when in the unconstrained region, the velocity is tuned to the optimal amplitude given by complex-conjugate control, as in (17). Otherwise, the maximum allowed velocity (lower than the optimal) is imposed, while keeping the velocity in phase with the excitation force. The control structure is illustrated in Figure 10. Since the algorithm is only loosely based on the WEC model, it has relatively good robustness to modeling error. Lower loop control, illustrated in Figures 9 and 10, is performed using internal model control (IMC) [60], while a robust servo controller was developed in [61]. The simple but effective (SE) controller, when compared with a model predictive controller (MPC) in both wide- and narrow-banded seas, has a relative capture width (RCW) within about 10% of the MPC (see Figure 11) and even outperforms the MPC for long wave periods in the low H_s case. Capture width is a common index of performance in wave energy and refers to the width of the wave front (assuming unidirectional waves) that contains the same amount of power as that absorbed by the WEC [62]. However, the simple controller has superior robustness to variations in K_b and has a relatively tiny fraction of the computational complexity of MPC. Note also, from Figure 11, that the amplitude and force limits of

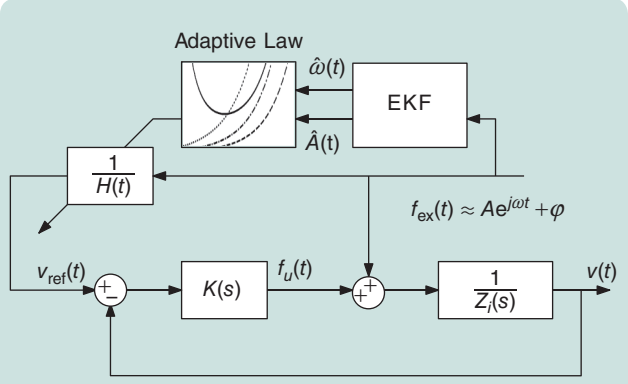

FIGURE 10 A proposed control architecture for the simple/effective controller. The extended Kalman filter effectively tracks the wave frequency and amplitude as in (18), while the $1/H(t)$ block provides an adaptive feedforward gain to determine the optimal velocity profile. $K(s)$ regulates the power take-off to ensure that the optimal velocity profile is achieved.

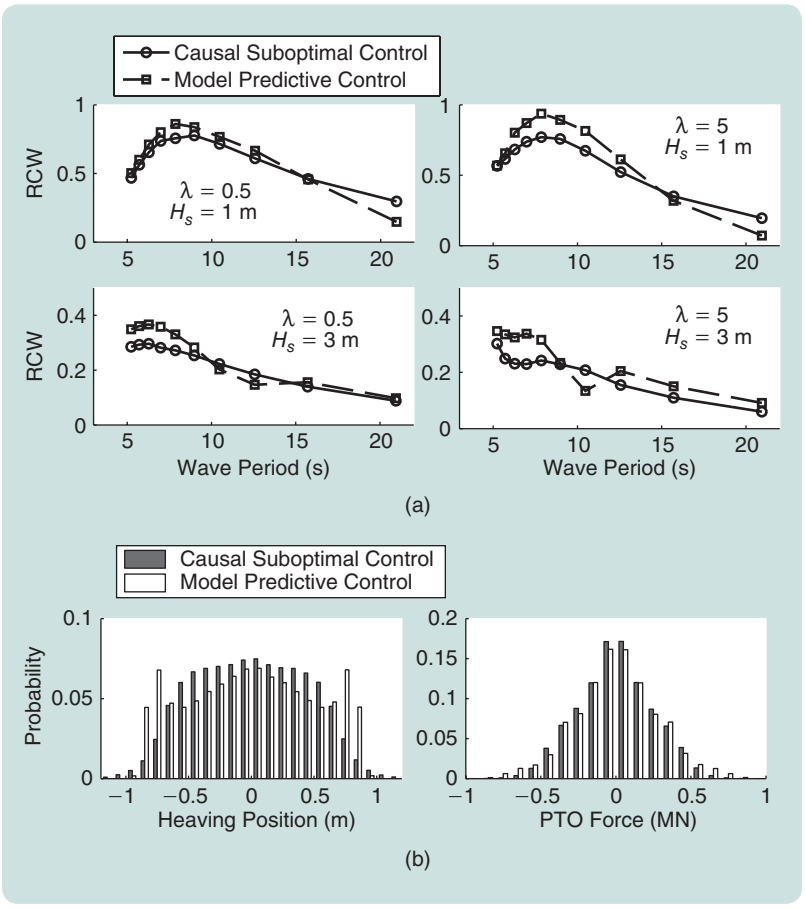

FIGURE 11 Performance of the suboptimal causal control, compared with model predictive control. Relative capture width (RCW) figures of merit are comparable for both controllers, with some small compromise on PTO force limits by the simple-but-effective controller. (a) RCW. (b) Distribution of heaving excursion and PTO force.

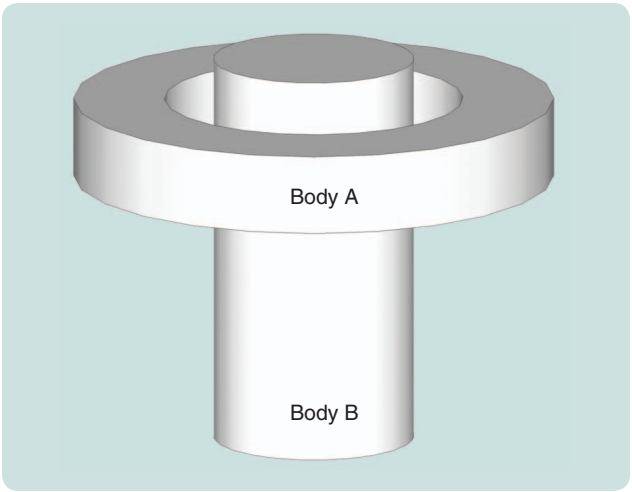

FIGURE 12 A two-body self-reacting device. Each body is tuned to a different resonant frequency, encouraging relative motion. The power take-off harnesses this relative motion. Typical examples include the Wavebob and OPT Powerbuoy devices.

±1 m and ±1 MN are, in general, well respected. The parameter λ in Figure 11 reflects the sea spectrum bandwidth ($\lambda = 0.5 \Rightarrow$ wide banded) from the Ochi sea spectrum model [18]. Further details and results for this controller are given in [63]. In a recent real-time implementation comparison [64], the SE controller outperformed an MPC controller, possibly due to the fact that the MPC was more heavily reliant on a mathematical model containing errors.

An MPC-Like Control Algorithm

The control solution presented in this section is based on the discretization, in the time domain, of the PTO force and of the motion of the device to transform the problem into a nonlinear program. The approach is similar to the direct simultaneous method used for the solution of optimal control problems [65], where both the control variables and the state variables are discretized. The main steps are documented here, with more complete details available in [66] and [67]. The application is the general two-body device shown in Figure 12. Consistent with the desire to maximize the converted energy, a performance function of the form

$$J(T) = \int_0^T f_{\text{pto}}(t)(v^A(t) - v^B(t))dt \qquad (26)$$

is specified, where the vertical velocities of body A and body B are denoted $v^A(t)$ and $v^B(t)$, respectively. The system model, which includes interactions between the two bodies, is

$$\begin{cases} L^A(t) = m^A\dot{v}^A(t) & +B^A v^A(t) + S^A u^A(t) \\ & -f_e^A(t) - f_r^A(t) + f_{\text{pto}}(t) = 0 \\ L^B(t) = m^B\dot{v}^B(t) & +B^B v^B(t) + S^B u^B(t) \\ & -f_e^B(t) - f_r^B(t) - f_{\text{pto}}(t) = 0 \end{cases}, \qquad (27)$$

where the hydrostatic buoyancy is described by S^A and S^B, while B^A and B^B are terms describing the linear viscous loss. The excitation forces on body A and body B are denoted by f_e^A and f_e^B, respectively. The objective is to find the optimal profile of the PTO force (f_{pto}) in a given time interval of length T that maximizes the absorbed energy $J(T)$ as defined in (26), subject to

$$\|u^A(t) - u^B(t)\|_\infty \le \Delta U_{\max}. \qquad (28)$$

The PTO force is assumed to be such that $f_{\text{pto}}(t) \in L^2([0,T])$, where $L^2([0,T])$ is the Hilbert space of square integrable functions in the interval $[0,T]$ and also $v^A(t), v^B(t) \in L^2([0,T])$ because these velocities are of physical bodies. The PTO force and the velocities are then approximated as a linear combination of basis functions in a finite-dimensional subspace of the space $L^2([0,T])$,

Much work remains to develop control strategies that perform well over the complete WEC operational space.

$$v^A(t) \approx \hat{v}^A(t) = \sum_{j=1}^{N} x_j^A \phi_j(t), \tag{29}$$

$$v^B(t) \approx \hat{v}^B(t) = \sum_{j=1}^{N} x_j^B \phi_j(t), \tag{30}$$

$$f_{\text{pto}}(t) \approx \hat{f}_{\text{pto}}(t) = \sum_{j=1}^{N^P} p_j \phi_j^p(t). \tag{31}$$

For any given set of coefficients describing the PTO force $\{p_1,\ldots,p_{N^P}\}$, the components of the velocities are calculated by solving the system

$$\begin{cases} \langle L^A(t), \phi_j \rangle = 0, \\ \langle L^B(t), \phi_j \rangle = 0, \end{cases} \text{for all } j = 1,\ldots N, \tag{32}$$

where $\langle \cdot, \cdot \rangle$ denotes the inner product. Using the approximations in (29)–(31) and choosing Fourier series for the basis, (27) can be written [66] as

$$\begin{bmatrix} G^{AA} & G^{AB} \\ G^{BA} & G^{BB} \end{bmatrix} \begin{bmatrix} X^A \\ X^B \end{bmatrix} = \begin{bmatrix} E^A \\ E^B \end{bmatrix} + \begin{bmatrix} -I_{2N} \\ I_{2N} \end{bmatrix} P, \tag{33}$$

where I_{2N} is the identity matrix of size $2N$, and

$$\begin{aligned} X^A &= [a_1^A, b_1^A, a_2^A, b_2^A, \ldots, a_N^A, b_N^A]^\top, \\ X^B &= [a_1^B, b_1^B, a_2^B, b_2^B, \ldots, a_N^B, b_N^B]^\top, \\ E^A &= [e_1^{A_c}, e_1^{A_s}, e_2^{A_c}, e_2^{A_s}, \ldots, e_N^{A_c}, e_N^{A_s}]^\top, \\ E^B &= [e_1^{B_c}, e_1^{B_s}, e_2^{B_c}, e_2^{B_s}, \ldots, e_N^{B_c}, e_N^{B_s}]^\top, \\ P &= [a_1^p, b_1^p, a_2^p, b_2^p, \ldots, a_N^p, b_N^p]^\top, \end{aligned}$$

where $E^{A,B}$ are the set of excitation force coefficients. The matrix

$$G = \begin{bmatrix} G^{AA} & G^{AB} \\ G^{BA} & G^{BB} \end{bmatrix}$$

contains hydrodynamic coefficients corresponding to the terms in (27). The performance function in (26) can now be rewritten as

$$J(P) = -P^\top H P + P^\top (Q^A E^A - Q^B E^B), \tag{34}$$

where H and $Q^{A,B}$ are functions of the elements of G. The matrix H can be shown to be positive definite; therefore, the quadratic cost function (34) is concave, and the global maximum of the *unconstrained* problem is obtained for

$$\bar{P} = (H + H^\top)^{-1} (Q^A E^A - Q^B E^B). \tag{35}$$

The constrained optimization problem

$$\max_P J(P) \text{ subject to } \|\Delta u\|_\infty \le \Delta U_{\max}, \tag{36}$$

is solved using the penalty method [68]; the constrained maximization problem (36) is therefore reformulated as the unconstrained minimization

$$\min_P -J(P) + \mu \max\{0, \|\Delta u\|_\infty - \Delta U_{\max}\}, \tag{37}$$

where $\mu > 0$ is the penalty parameter. The optimization is solved by starting with $\mu_1 \ll 1$, which corresponds to the unconstrained problem; if the solution violates the constraint, then μ_k is updated as $\mu_{k+1} = \alpha \mu_k$ with $\alpha > 1$ and the new solution P_{k+1}^* is calculated. If the constraint is satisfied, the algorithm stops, otherwise the process is repeated until the solution is found.

For this control study, the feedback controller, as shown in Figure 9, was obtained by solving a continuous-time linear-quadratic (LQ) tracking problem. Figure 13 shows sample results for the energy-maximizing controller, where the controller is switched on between $t = 100$ and $t = 375$ s. The normalized amplitude constraint is 0.1 m for this simulated example.

Other MPC-like WEC control algorithms have been presented in [69]–[71]. A chief difficulty in applying MPC to a performance function of the form of (26) is that the performance function is, in general, nonconvex. The closely related optimal LQ Gaussian (LQG) problem for wave-energy devices has been studied in [72].

Overview of the WEC Control Literature

This section provides an overview of the literature on the control of WECs and wave-energy arrays (farms). As a starting point, reviews of wave-energy conversion in general terms in [73]–[80] provide a historical review of the

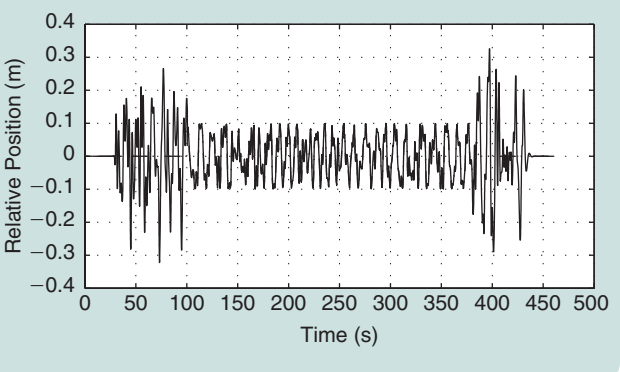

FIGURE 13 Evolution of the relative position for the MPC-like controller. The relative position constraint is strictly observed over the control period.

Dynamic analysis and control system technology can impact many aspects of WEC design and operation.

control of WECs. A special issue of the *Philosophical Transactions of the Royal Society* on wave energy also provides a good overview of control of WECs [81].

Several publications compare control strategies. While latching (see "Discrete Control—Latching and Declutching") is suboptimal, this control strategy generally provides significant improvements with respect to passive control as shown, for example, in [82] and [83]. More detailed comparisons between optimal control, latching, and passive control are reported in [84]–[86] for both model simulations and wave tank tests.

For a simulated two-body device, reactive phase control resulted in significantly higher converted energy than latching control, and latching did not provide a significant improvement over a passive linear damper [87], in contrast to the boost observed in the single-body case. Several control techniques have been applied to the first Archimedes wave swing (AWS) prototype, with performance comparisons reported in [88]–[90]. The control algorithms implemented are reactive control, phase and amplitude control, latching, IMC, and feedback linearization. Control methods for a heaving point absorber have been reviewed in [91], and control strategies for the Wavestar device have been compared with respect to the mechanical fatigue that they generate [54].

Finally, the Ph.D. theses [28], [92], [93], and [67] provide a good overview of wave-energy devices, their control, and associated issues.

Fundamental Results

The analytical formulation for the maximum power absorbed by a system of oscillating devices was originally derived, independently, in [94] and [95]. Overviews of optimal control theory for heaving-body WECs are provided in [80], [96], and [97]. Reference [29] gives a comprehensive description and discussion about the theory of maximum power absorption, while [98] also provides an overview of the theory of WEC optimal control, with a time-domain formulation of the optimality problem and a solution for a motion-compensated platform on a floating body in an irregular sea.

One of the first applications of reactive control is described in [99] and applied to the Salter duck, which was a pioneering WEC device developed in the 1970s. Complex-conjugate control, applied to the Salter duck, is also described in [100]. Simulation and experimental results showed the device "can absorb 100% of the incident power in its own width for linear monochromatic waves" [100] in a certain frequency band. Reactive (complex-conjugate) control has been implemented for a semisubmerged sphere oscillating in heave [101].

Complex conjugate control for a single DoF heaving-body-type WEC is presented in [53] and [102], where the buoy is directly coupled to a linear generator. A two-body coupled oscillator is considered in [103] and [104] and a frequency-domain model for the 2-DoF system is presented. A study of optimal control applied to a two-body point absorber oscillating in heave is also described in [105].

The effect of irregular waves (polychromatic waves) on complex-conjugate control is analyzed in [106] and [107], while signal processing techniques are applied in [108] to irregular wave measurements to mitigate the effect of anticausality and improve power absorption when implementing reactive control.

Causal Control

In [109] and [110], reactive control of a WEC using a linear generator is implemented by tuning the PTO to the peak wave frequency. The WEC is then described by a second-order differential equation with frequency *independent* coefficients. A similar approach is described in [111]. Implementation of causal control for the Wavestar WEC device is described in [112].

In [113], the noncausal transfer function between the optimal velocity and the excitation force is approximated by a constant. It is claimed that, while significantly reducing the complexity and improving the robustness of reactive control, the energy capture was nearly optimal. Details and performance analysis of the controller in [113] are given in the section "Simple but Effective Control." A different approach is presented in [114] and [115], where an optimal causal control system is developed for a 3-DoF (surge, pitch, and heave) WEC based on an LQG regulator, which obviates the causality issue. Causal stochastic optimal control is implemented in [116], where the proportionality coefficient between the body velocity and the control signal is frequency independent and was obtained by means of an optimization based on the spectral characteristics of the wave elevation.

Linear PTO Damping

Linear PTO damping parameterizes the PTO force as $f_{\text{pto}}(t) = -\text{B}_{\text{pto}} v(t)$, where B_{pto} is the PTO damping coefficient. The optimal value of B_{pto}, which maximizes the instantaneous absorbed power, was calculated for a monochromatic incident wave in [29]. Damping optimization for a vertical cylinder heaving WEC, for both regular and irregular seas, was carried out in [117]. Damping optimization has

A strong interaction between the optimal WEC array layout and the control algorithm employed has been demonstrated.

also been studied also for a similar device subject to constraints [118].

Reference [119] compared several passive tuning (constant B_{pto}) strategies for irregular seas, whereas damping optimization is considered in [120]. A two-body heaving WEC is considered in [121], where damping coefficients for several wave climates are optimized. Experimental results from sea trials for a linear damping are provided in [122], while the experimental and simulation results are compared for the same device in [123] and with a small mass modification in [124]. The study is further extended in [125] and [126] by considering the influence of damping on absorbed power for different sea states.

A slight variation on linear damping for the Wavebob device is considered in [127], where the performance of two different type of hydraulic circuits are compared, with a constant damping force when the velocity is larger than a threshold. A WEC with hydraulic PTO is also considered in [128] and [129], where the damping was optimized in regular and irregular seas, with the displacement of the hydraulic motor controlling the damping.

Other Control Strategies

In [130] and [88], feedback linearization control and IMC, with both linear and neural networks models, are applied to the AWS device. The work was extended in [131] to include a switching controller that selects the appropriate control strategy based on the sea state.

An instantaneous control algorithm for a two-body WEC with a hydraulic PTO is implemented in [132], consisting of a linear relationship between the hydraulic motor flow and the pressure applied on the piston. This highly nonlinear PTO mechanism was demonstrated to attain very nearly the same level of wave-energy extraction as an optimally controlled fully linear mechanism. A parameter optimization for a generic vertical cylinder WEC with respect to wave climate is described in [133].

Fuzzy logic control has also been used for the control of WECs. For instance, fuzzy logic is used to adjust PTO damping and stiffness based on the sea state and the instantaneous wave profile in [134]. As an extension, fuzzy logic, genetic algorithms, and robust control were combined in [135] and [136]. Genetic algorithms have also been used, in conjunction with neural control, for the design of a causal latching control strategy [137]. A WEC equipped with a hydraulic PTO was considered in [138], where the fuzzy controller was designed to adjust the hydraulic pump displacement, with the objective of regulating the speed of the electric generator shaft to the setpoint, which maximizes the conversion efficiency of the overall energy absorption. An additional example of fuzzy logic applied to the control of WECs can be found in [139], while the work in [140] describes a control strategy based on a multiobjective particle swarm optimization technique.

PTO damping and spring coefficients of a self-reacting heaving WEC have been optimized by a stochastic approach using Pontryagin's maximum principle [141], [142]. The control system presented in [143] is composed of high- and low-level controllers. The high-level controller generates a PTO damping reference, while the low-level controller is of the proportional integral plus (PIP) form, implemented as feedforward PIP and state-dependent PIP [144]. The high-level optimization of captured energy is based on evolutionary algorithms [145].

Losses of the hydraulic PTO have been considered for a point absorber WEC [146], [147]. Efficiency of the hydraulic PTO has been studied in [148] as part of an effort to optimize the passive damping and maximize the absorbed energy for the Wavebob device. PTO efficiency issues are also considered for a range of control strategies in [149].

In [150], a maximum-power, point-tracking algorithm is employed for the control of a point-absorber WEC equipped with a linear electrical generator. Control of WECs has also been performed by adjusting the inertia of the system [151], where mechanical amplification of oscillations are pursued by means of mass modulation, implemented by using water as ballast. A different approach for the control of the inertia of the absorbing system is to adjust the natural frequency of the WEC by repositioning an internal mass [152].

The reduction of parametric resonance for a heaving buoy WEC was investigated in [36], while filter design principles were used to implement a wide bandwidth controller in [153] to improve the independence of WEC absorption performance from the sites in which they are deployed.

When the conditions of the sea become too severe, control systems are generally programmed to shut down the device to protect the WEC. A control strategy called quiescent-period predictive control has been claimed to increase the average annual power production by preventing the control system from unnecessarily deactivating the device [154], [155].

For other control strategies based on forms of discrete (switching) control, see "Discrete Control—Latching and Declutching."

Constrained Control

Several researchers have studied the problem of maximizing the absorbed energy under the effect of constraints on

A broad range of control technologies and algorithms have strong potential in the area of wave-energy control.

the motion of the oscillating body, or on the maximum PTO forces. In [156], the power absorption capabilities of a slender body with motion restrictions is studied. Subsequently, [157] presented a theory for the maximization of wave-power absorption of a system of oscillating bodies in the frequency domain subject to oscillation amplitude restrictions. A more general formulation is provided in [158], where the author removes the limitation of having the same amplitude restriction on all degrees of freedom.

In [151], the oscillation amplitude constraints are enforced by increasing the PTO damping, while [159] formulates an optimization problem in the frequency domain considering a WEC where energy is absorbed by means of the relative oscillation between a floating body and an on-board actively controlled motion-compensated platform. The constraint on the amplitude of the relative oscillation is introduced as a penalty term in the cost function to describe the balance between absorbed energy and oscillation amplitude.

The maximization of the absorbed energy with motion and force restrictions has also been considered from a probabilistic standpoint in [118], with a heaving-point absorber moving with respect to a floating reference. The buoy is subject to restrictions on the relative oscillation amplitude due to the finite length of the stroke and to avoid slamming. The work was extended in [160] where the same analysis has been carried out for a small array of WECs. Reference [161] implements LQG control, applied to a 3-DoF WEC, with constraints on the PTO force, displacement, and voltage and current of the electrical generator, with the constraints formulated in terms of variance.

An early time-domain formulation for (amplitude) constrained maximization of absorbed energy is described in [162], where the WEC is a heaving cylinder subject to both regular and irregular (polychromatic) waves.

A powerful tool for the real-time optimal control of constrained systems is MPC, which has been used in the context of wave-energy conversion [163]–[167]. In [163], the influence of the excitation force prediction horizon on the

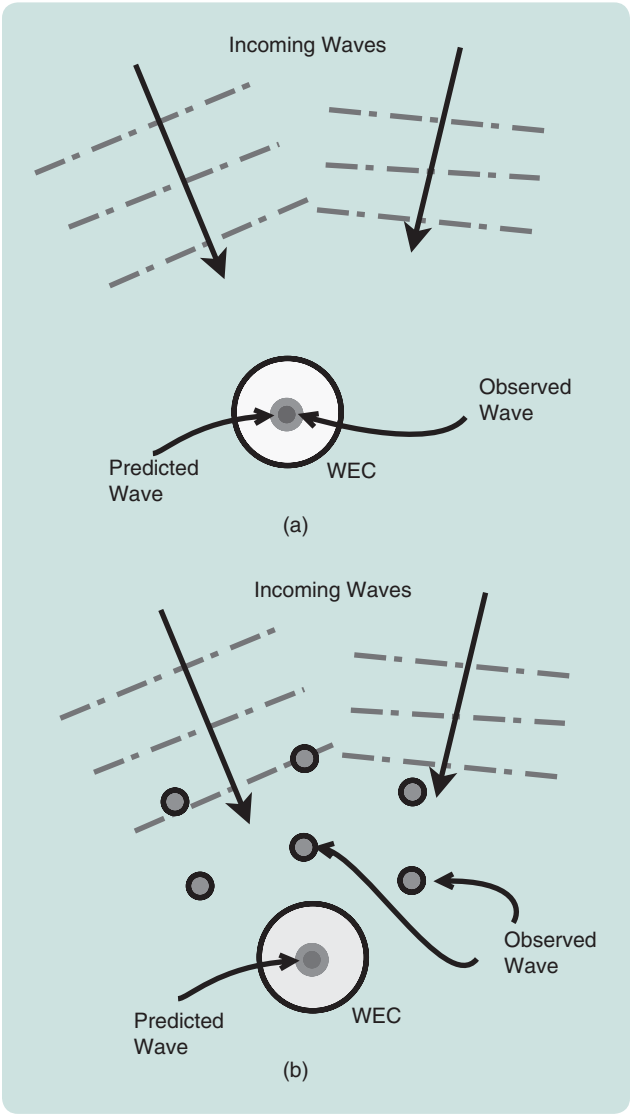

FIGURE 14 The two main approaches to wave forecasting. Up-wave prediction requires the addition of extra sensors, while the time series approach in (a) simply forecasts future excitation force based on the measured device motion. (a) Prediction based only on local single-point measurements. (b) Prediction based on up-wave measurements.

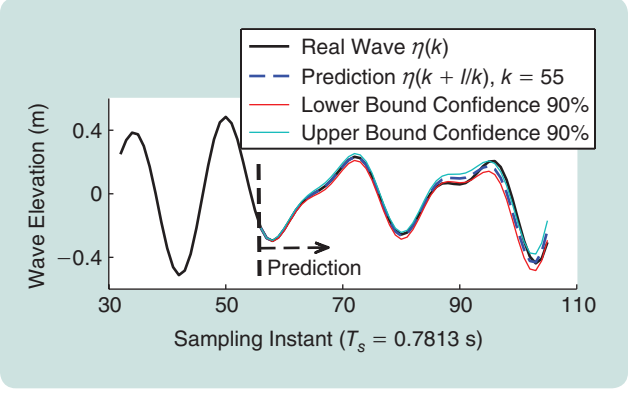

FIGURE 15 Wave prediction and confidence intervals for a filtered wave record for Pico Island in the Azores. The prediction shows acceptable fidelity over a 35-s forecast horizon.

absorbed energy is examined, whereas [164] has described an improved formulation of MPC compared to [163], which has more favorable structural properties that facilitate online implementation. MPC has been implemented on a simple point absorber, with constraints on velocity, position, and generator force [165], and where the prediction of the excitation force was performed by a Kalman filter. Nonlinear MPC has also been implemented in [168] on a generic WEC and in [166] on a two-body heaving point-absorber, where the hydrodynamic model of the device is linear and the nonlinearities are due to mooring forces.

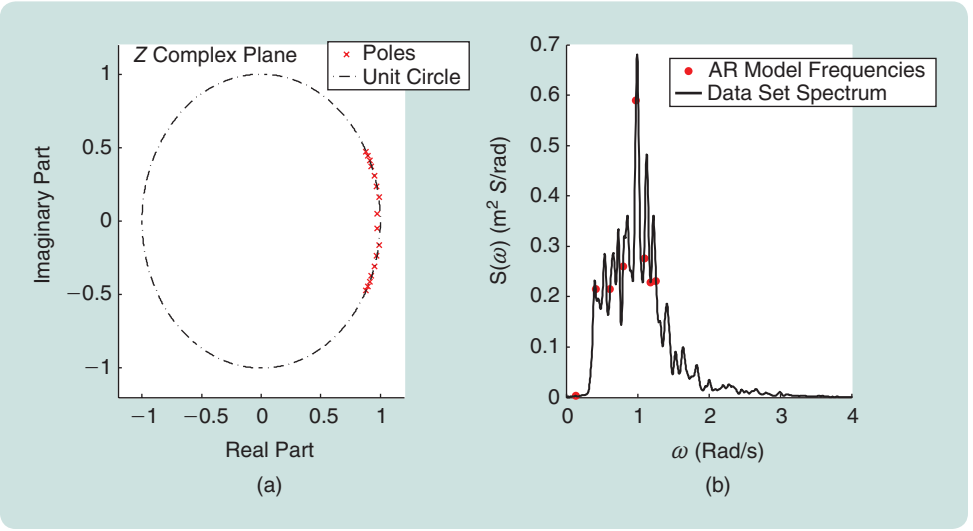

FIGURE 16 Autoregressive (AR) model poles and the corresponding sea spectrum. Though the AR model is essentially a time-domain model, the pole locations give a useful frequency-domain interpretation, which can be related to the sea spectrum.

Control of Wave Farms

The analytical formulation of the maximum power absorbed by an array of oscillating devices was independently derived in [94] and [95]. Both researchers obtained a result that is the general case of reactive (phase and amplitude control) control. A *system* of optimally controlled WECs is described in [157], which also considered the effect of motion constraints on maximum power absorption. Also, [169] reports a study on linear arrays of heaving buoys, where unconstrained motion as well as constrained motion is considered. The work of [169] is extended in [170], which considered an infinite linear array of evenly spaced oscillating bodies. Constraints on arrays of oscillating bodies were considered in [171], where limiting the oscillation amplitude to two or three times the incoming wave amplitude results in the positive interference between array elements being reduced, although the negative interference is not significantly affected.

Reference [172] presents a suboptimal method for the control of an array of WECs to obviate the issue associated with knowledge of the velocities of all devices, when calculating the optimal force for each device. A comparison between reactive control and suboptimal control is reported in [173], where suboptimal control is implemented by taking the diagonal of only the real part of the optimal PTO impedance matrix, resulting in the linear damping terms only. Several suboptimal control strategies are studied in [174], where two array configurations are considered, with both comprising five bodies in linear cross-shaped arrays. A similar approach is presented in [175] and [176] for a square array of vertical cylinders. As in [174], the damping is optimized both independently for each device and also globally, imposing the same value for all the devices. In [177], the damping for an array of four heaving hemispherical devices is optimized for each frequency.

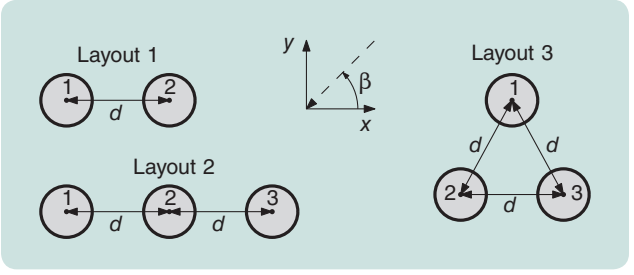

FIGURE 17 Wave-energy converter array layouts relative to the incident wave angle, β. All layouts are defined have a single separation parameter d.

Arrays of WECs are considered in [178] and [179] for PTOs with both damping and spring terms. The PTO tuning is equal for each device in the array and corresponds to the optimal tuning for an isolated WEC, as also in [180] and [181].

Independently optimized damping for each device is implemented in [182], where the array is composed of five closely spaced, aligned, heaving hemispheres. Constrained control of an array of 12 closely spaced, heaving-point absorbers is studied in [183] and [184], where the interbody distance is just 1.3 times the diameter of the WEC. An array of two heaving cylinders with a nonlinear PTO is considered in [185], where several values of the hydraulic precharge pressure are compared, to find an optimal relation between PTO precharge pressure and incident wave period.

Finally, a real-time control algorithm for arrays of WECs, using a basis function parameterization of system variables (following the general development in the section "An MPC-Like Control Algorithm"), is presented in [47], and the

method is extended to consider system constraints in [34]. An MPC algorithm, using an approximate cost function, is presented in [71] and applied to control arrays of WECs.

WAVE FORECASTING

While some WEC control algorithms circumvent the need to predict future variations in free surface elevation or excitation force [63], [72], in general there is a need to provide forecast values of free surface elevation or excitation force due to the noncausality of the optimal PTO force, as articulated in the section "Wave-Energy Control Fundamentals." Fortunately, there is a strong positive connection between the wave forecasting requirements of energy-maximizing control [92] and the forecastability of random seas [59], due to the close relationship between the radiation damping dynamics and the design sea state (the predominant wave period).

Wave forecasting can be performed using up-wave measurement [186]–[189] or time-series modeling at the device location [59], as shown in Figure 14. A comparative case study [190] has demonstrated little benefit in including up-wave measurements in forecasting the variations in the water column of an OWC compared to autoregressive (AR) methods, which are based purely on historical measurements of the water column variations. However, the generality of such a result is not proven. While many time-series techniques may be employed, including harmonic models, neural network models, and models based on the EKF, a simple linear AR forecasting model such as

$$\hat{\eta}(k+l \mid k) = \sum_{i=1}^{n} \hat{a}_i(k)\,\hat{\eta}(k+l-i \mid k) \tag{38}$$

performs well and has a convenient frequency-domain interpretation. As an example, Figure 15 shows $\hat{\eta}(k+l \mid k)$, for $l = 1$ to $l = 50$, at a specific time instant k, calculated with an AR model of order $n = 24$ on the data set P_2, filtered with cutoff frequency $\omega_c = 0.7$ rad/s for wave data at Pico Island in the Azores. Figure 16 shows how the AR model poles pick out the characteristic spectral peaks in the sea spectrum.

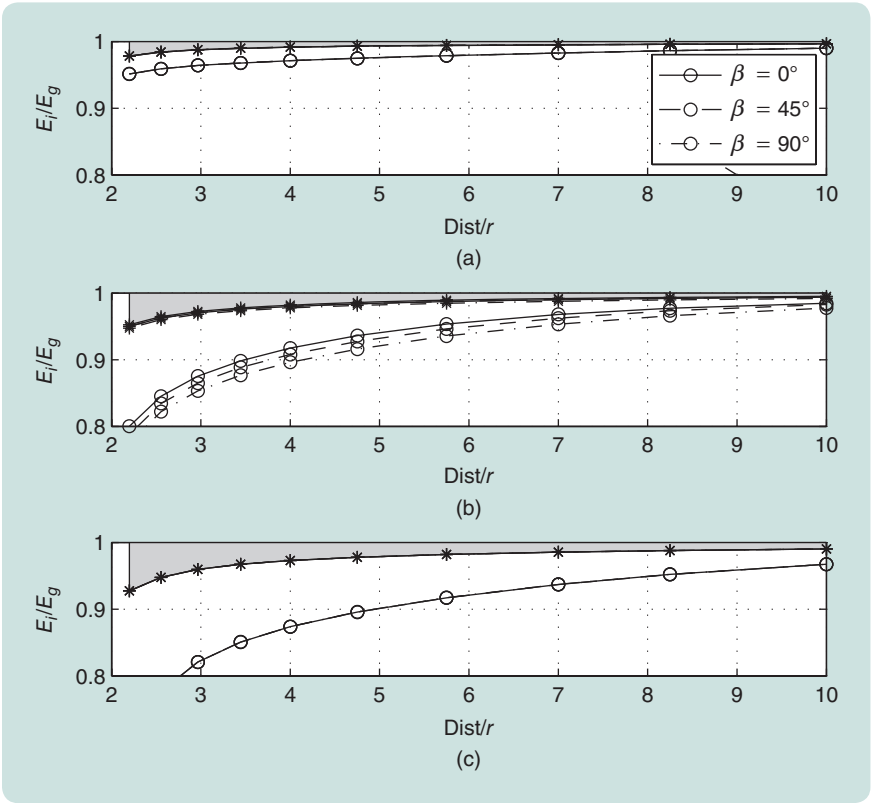

FIGURE 18 The relative performance of the independent and global controllers for an array of heaving cylinders. In some cases, energy capture improvement of 10–20% can be obtained through the use of a global controller, compared to independent control. (a) Layout 1. (b) Layout 2. (c) Layout 3.

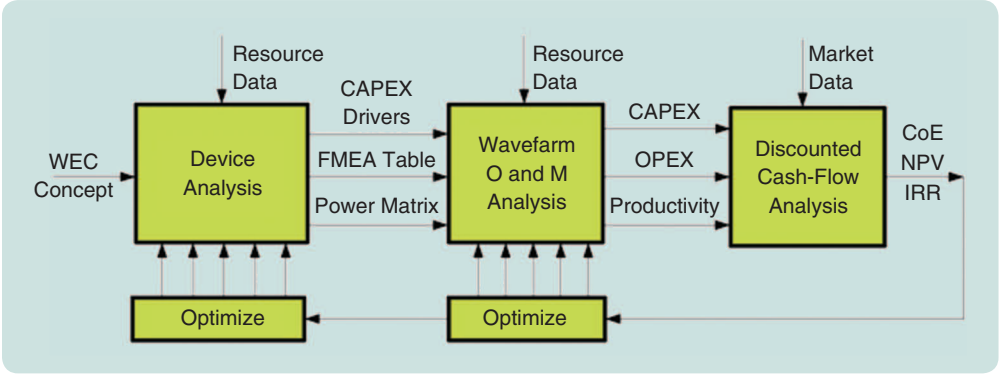

FIGURE 19 Technoeconomic optimization. Significant computation is involved, including the required recalculation of hydrodynamic parameters in the "device analysis" block, as the wave-energy converter geometry is adapted.

CONCLUSIONS AND PERSPECTIVES

Researchers from a variety of disciplines have addressed the wave-energy control problem since the 1970s. However, much work remains to develop control strategies that perform well

It is already clear that appropriate control technology has the capability to double the energy taken from WECs.

over the complete WEC operational space, are insensitive to modeling errors and disturbances, and have some fault-tolerant capability since WECs are normally located in remote areas. It is estimated that, for wave farms, maintenance costs are likely to be the same order of magnitude as capital costs.

There are many new promising areas where control can make further contributions in wave-energy applications, including cooperative control of arrays of wave-energy devices [47], [34], [71]. For example, for the sample array layouts of Figure 17, Figure 18 shows the ratio (E_i/E_g) of energy captured by an array of heaving cylinders (radius = 4 m, draft = 10 m, resonance period = 7.1 s) with independent device control (E_i) and global coordinated control (E_g) in a sea with peak period $T_p = 12$ s $(\lambda = 225\,\text{m})$. The optimal control laws (roughly based on the algorithm in the section "An MPC-Like Control Algorithm") for each WEC, in the case of independent control (IC), are obtained by iteration, during which time the estimator and predictor on each WEC builds up a reliable forecast of the incoming waves (reaching quasi-steady state). This asymptotic condition is denoted by the lines marked with * in Figure 18 and show the upper performance bound for the IC case, although such performance is not achievable in practice. For a more realistic comparison, global control (GC) and IC are evaluated considering only the first iteration of the IC (marked with °). The GC is based on the algorithm in the section "An MPC-Like Control Algorithm" but with the control model accounting for all hydrodynamic interactions between devices in the array, resulting in up to 20% better energy capture than IC.

An important consideration is the strong interaction between the ideal WEC geometric shape and the WEC control strategy employed [191]. In addition, a strong interaction between the optimal WEC array layout and the control algorithm employed has been demonstrated [192]. These system interactions have led to the consideration of total wave-energy system optimization, or technoeconomic optimization [193], illustrated in Figure 19, with the realization that, while energy or efficiency maximization is an interesting academic and engineering problem, the most important metric for a wave-energy system is the total economic benefit. However, articulation of detailed capital and operational costs for wave-energy systems is nontrivial [194]. To date, the wave-energy control problem has not received the full attention of the wider control systems community. A broad range of control technologies and algorithms have strong potential in the area of wave-energy control. In addition, some application areas that are relatively mature, from a control perspective, bear a strong resemblance to the wave-energy control problem. For example, the connection with wind turbine control was articulated in the section "Wave-Energy Control Fundamentals." The control of wave-energy devices is indeed a fertile control systems playground.

ACKNOWLEDGMENTS

This work was partly funded by the Irish Research Council (Embark Initiative), Enterprise Ireland (Grant TD/2009/0331), and Science Foundation Ireland (Grant 12/RC/2302 for the Marine Renewable Ireland [MaREI] Centre).

AUTHOR INFORMATION

John V. Ringwood (john.ringwood@eeng.nuim.ie) received the honors diploma from the Dublin Institute of Technology and the B.Sc.(Eng.) from the University of Dublin, Trinity College, both in electrical engineering, in 1981. He completed a Ph.D. in control systems engineering at Strathclyde University in 1984 and received a master's in music technology degree from the National University of Ireland (NUI), Maynooth, in 2005. Over the period 1985–2000, he held various academic positions at Dublin City University and has been a professor of electronic engineering at NUI, Maynooth, since 2000. He has held visiting positions at both Massey University and the University of Auckland in New Zealand. He was head of the Department of Electronic Engineering at NUI, Maynooth, from 2000 to 2006, developing the department from a greenfield site, and served as dean of engineering from 2001 to 2013. His current research interests include mathematical modeling and control systems and their application in wave energy, semiconductor manufacture, power converters, and exercise physiology. He is a chartered engineer, a Fellow of Engineers Ireland, and a Senior Member of IEEE. He can be contacted at the Department of Electronic Engineering, NUI, Maynooth, Co. Kildare, Ireland.

Giorgio Bacelli received the laurea magistrale in electronic engineering from Universitá Politecnica delle Marche, Italy, in 2006, and he completed a Ph.D. in electronic engineering at the Center for Ocean Energy Research at the National University of Ireland, Maynooth, in 2014. During his Ph.D., he worked on the modeling and control of wave-energy converters, with particular focus on numerical optimal control and modeling of multibody constrained systems.

Francesco Fusco received the master in industrial automation engineering degree from the Università Politecnica

delle Marche, Ancona, Italy, in 2008. He completed a Ph.D. in electronic engineering at the Center for Ocean Energy Research at the National University of Ireland, Maynooth, in 2012, with his work on forecasting and control of wave-energy converters. Since 2012, he has been a research scientist with the Smarter Cities Technology Centre, IBM Research Ireland. His current research interests include data analytics, fault diagnosis, and control of energy and water networks.

REFERENCES

[1] F. Fusco, G. Nolan, and J. V. Ringwood, "Variability reduction through optimal combination of wind/wave resources—An Irish case study," *Energy*, vol. 35, no. 1, pp. 314–325, 2010.

[2] M. McCormick, *Ocean Wave Energy Conversion*. New York: Wiley, 1981.

[3] H. Knight, "Edison's revenge," *New Sci*., vol. 200, no. 2677, p. 40, 2008.

[4] T. Thorpe, "An overview of wave energy technologies," ETSU, Tech. Rep., 1998.

[5] H. Soerensen, "Development of wave dragon from scale 1:50 to prototype," in *Proc. 5th European Wave Energy Conf.*, 2003, pp. 110–116.

[6] R. Yemm, D. Pizer, and C. Retzler, "Floating apparatus and method for extracting power from sea waves," U.S. Patent 6 476 511, Nov. 5, 2002.

[7] T. Whittaker and M. Folley, "Near-shore oscillating wave surge converters and the development of Oyster," *Philos. Trans. R. Soc. A*, vol. 370, pp. 345–364, Dec. 2012.

[8] M. Kramer, L. Marquis, and P. Frigaard, "Performance evaluation of the Wavestar prototype," in *Proc. 10th European Wave Tidal Energy Conf.*, Southampton, U.K., 2011.

[9] K. Koca, A. Kortenhaus, H. Oumeraci, B. Zanuttigh, E. Angelelli, M. Cantu, R. Suffredini, and G. Franceschi, "Recent advances in the development of wave energy converters," in *Proc. 9th European Wave Tidal Energy Conf.*, Aalborg, Denmark, 2013.

[10] B. Drew, A. Plummer, and M. Sahinaya, "A review of wave energy converter technology," *Proc. Inst. Mech. Eng. A, Power Energy*, vol. 223, no. 8, pp. 887–902, 2009.

[11] A. Babarit and J. Hals, "On the maximum and actual capture width ratio of wave energy converters," in *Proc. 10th European Wave Energy Conf.*, Southampton, U.K., 2011.

[12] J. Weber, R. Costello, and J. Ringwood, "WEC technology performance levels—Metric for successful development of economic WEC technology," in *Proc. 11th European Wave Energy Conf.*, Aalborg, Denmark, 2013.

[13] A. Babarit and A. Clement, "Optimal latching control of a wave energy device in regular and irregular waves," *Appl. Ocean Res*., vol. 28, no. 2, pp. 77–91, 2006.

[14] G. Bacelli, J. Ringwood, and J.-C. Gilloteaux, "Control of a wave energy device for potable water production," in *Proc. European Control Conf.*, 2009, pp. 3755–3760.

[15] C. Bretschneider, "The generation and decay of wind waves in deep water," *Trans. Amer. Geophys. Union*, vol. 33, no. 3, pp. 381–389, 1952.

[16] W. Pierson and L. Moskowitz, "A proposed spectral form for fully developed wind seas based on the similarity theory of S. A. Kitaigorodskii," *J. Geophys. Res*., vol. 69, no. 24, pp. 5181–5190, 1964.

[17] K. Hasselmann, T. P. Barnett, E. Bouws, H. Carlson, D. E. Cartwright, K. Enke, J. A. Ewing, H. Gienapp, D. E. Hasselmann, P. Kruseman, A. Meerburg, P. Müller, D. J. Olbers, K. Richter, W. Sell, and H. Walden, "Measurements of wind-wave growth and swell decay during the joint north sea wave project," Erganzungsheft zur Deutschen Hydrographischen Zeitschrift, Deutschen Hydrographischen Inst., Hamburg, Germany, Tech. Rep. Reihe A (8^0), Nr. 12, 1973.

[18] M. K. Ochi, *Ocean Waves: The Stochastic Approach*. Cambridge, U.K.: Cambridge Univ. Press, 1998.

[19] ESB International, "Accessible wave energy resource atlas: Ireland," Marine Inst./Suatainable Energy Ireland, Galway, Ireland, Tech. Rep. 4D404A-R2, 2005.

[20] J.-C. Gilloteaux and J. Ringwood, "Influence of wave directionality on a generic point absorber," in *Proc. 8th European Wave Tidal Energy Conf.*, Uppsala, Sweden, 2009, pp. 979–988.

[21] G. Nolan, J. Ringwood, and B. Holmes, "Short term wave energy variability off the West Coast of Ireland," in *Proc. 7th European Wave Tidal Energy Conf.*, Porto, 2007.

[22] C. Josset, A. Babarit, and A. H. Clement, "A wave-to-wire model of the SEAREV wave energy converter," *Proc. Inst. Mech. Eng. M, J. Eng. Maritime Environ*., vol. 221, no. 2, pp. 81–93, 2007.

[23] P. Cleary, M. Prakash, J. Ha, N. Stokes, and C. Scott, "Smooth particle hydrodynamics: Status and future potential," *Progr. Comput. Fluid Dyn*., vol. 7, nos. 2–4, pp. 70–90, 2007.

[24] E. B. Agamloh, A. K. Wallace, and A. von Jouanne, "Application of fluid structure interaction simulation of an ocean wave energy extraction device," *Renew. Energy*, vol. 33, no. 4, pp. 748–757, 2008.

[25] J. Davidson, S. Giorgi, and J. Ringwood, "Linear parametric hydrodynamic models based on numerical wave tank experiments," in *Proc. 9th European Wave Tidal Energy Conf.*, Aalborg, Denmark, 2013.

[26] M. Trapanese, "Optimization of a sea wave energy harvesting electromagnetic device," *IEEE Trans. Magn*., vol. 44, no. 11, pp. 4365–4368, 2008.

[27] G. Bacelli, J.-C. Gilloteaux, and J. Ringwood, "State space model of a hydraulic power take off unit for wave energy conversion employing bondgraphs," in *Proc. World Renewable Energy Conf.*, Glasgow, U.K., 2008.

[28] J. Hals, "Modelling and phase control of wave energy converters," Ph.D. dissertation, Dept. Eng. Cybern., Norwegian Univ. Sci. Technol., Trondheim, Norway, 2010.

[29] J. Falnes, *Ocean Waves and Oscillating Systems*. Cambridge, U.K.: Cambridge Univ. Press, 2002.

[30] W. Cummins, "The impulse response function and ship motions," *Schiffstechnik*, vol. 9, pp. 101–109, Oct. 1962.

[31] *WAMIT User Manual*, WAMIT Inc., Chestnut Hill, MA, 2002.

[32] A. Clement, "Using differential properties of the green function in seakeeping computational codes," in *Proc. European Control Conf.*, 2009, pp. 3755–3760.

[33] G. Bacelli and J. Ringwood, "A geometric tool for the analysis of position and force constraints in wave energy converters," *Ocean Eng*., vol. 65, pp. 10–18, June 2013.

[34] G. Bacelli and J. Ringwood, "Constrained control of arrays of wave energy devices," in *Proc. 11th European Wave Energy Conf.*, Aalborg, Denmark, 2013.

[35] S.-C. Lee, "A finite element boundary element method for infinite periodic structures on non-periodic meshes using an interior penalty formulation," Ph.D. dissertation, Electr. Comput. Eng., Ohio State Univ., Columbus, OH, 2012.

[36] C. Villegas and H. van der Schaaf, "Implementation of a pitch stability control for a wave energy converter," in *Proc. 10th European Wave Tidal Energy Conf.*, Southampton, U.K., 2011.

[37] R. Beck and A. Reed, "Modern computational methods for ships in a seaway," *Trans. Soc. Naval Arch. Marine Eng*., vol. 109, pp. 1–52, 2001.

[38] J. de Kat and R. Pauling, "The simulation of ship motions and capsizing in severe seas," *Trans. Soc. Naval Arch. Marine Eng*., vol. 97, pp. 139–168, Jan. 1989.

[39] R.-Q. Lin and W. Kuang, "A fully nonlinear, dynamically consistent numerical model for solid-body ship motion. I. ship motion with fixed heading," *Proc. Royal Soc. A: Math. Phys. Eng. Sci*., vol. 467, no. 2128, pp. 911–927, 2011.

[40] J.-C. Gilloteaux, "Simulation de mouvements de grande amplitude—Application a la récupération de l'energie des vagues," Ph.D. dissertation, Laboratoire de recherche en Hydrodynamique, Énergétique et Environnement Atmosphérique, Ecole Centrale de Nantes, Nantes, France, 2007.

[41] J.-C. Gilloteaux, G. Bacelli, and J. V. Ringwood, "A non-linear potential model to predict large-amplitudes-motions: Application to a multi-body wave energy converter," in *Proc. 10th World Renewable Energy Conf.*, 2008, pp. 934–939.

[42] A. Merigaud, J.-C. Gilloteaux, and J. Ringwood, "A nonlinear extension for linear boundary element methods in wave energy device modelling," in *Proc. Int. Conf. Offshore Mechanics Arctic Engineering*, Rio de Janeiro, 2012.

[43] M. Guerinel, M. Alves, and A. Sarmento, "Nonlinear modelling of the dynamics of a free floating body," in *Proc. 10th European Wave Tidal Energy Conf.*, Southampton, U.K., 2011.

[44] J. R. Morison, M. P. O'Brien, J. W. Johnson, and S. A. Schaaf, "The force exerted by surface waves on piles," *Trans. AIME Petr*., vol. 189, no. 5, pp. 149–154, 1950.

[45] M. Bhinder, A. Babarit, L. Gentaz, and P. Ferrant, "Effect of viscous forces on the performance of a surging wave energy converter," in *Proc. Conf. Int. Society Offshore Polar Engineers*, 2012, pp. 545–550.
[46] Z.-D. Yuan and Z.-H. Huang, "An experimental study of inertia and drag coefficients for a truncated circular cylinder in regular waves," *J. Hydrodyn.*, vol. 22, no. 5, pp. 318–323, 2010.
[47] G. Bacelli, P. Balitsky, and J. Ringwood, "Coordinated control of arrays of wave energy devices—Benefits over independent control," *IEEE Trans. Sust. Energy*, vol. 4, no. 4, pp. 1091–1099, 2013.
[48] T. Perez and T. Fossen, "Time-domain models of marine surface vessels for simulation and control design based on seakeeping computations," in *Proc. 7th IFAC Conf. Manoeuvring Control Marine Craft*, 2006.
[49] A. P. McCabe, A. Bradshaw, and M. B. Widden, "A time-domain model of a floating body using transforms," in *Proc. 6th European Wave Tidal Energy Conf.*, Glasgow, U.K., 2005.
[50] E. Levy, "Complex curve fitting," *IRE Trans. Autom. Contr.*, vol. 4, no. 1, pp. 37–43, 1959.
[51] R. Prony, "Essai experimental et analytique: Sur les lois de la dilatabilite des fluides elastiques et sur celles de la force expensiver de la vapeur del'eau et de la vapeur de l'alkool, a differentes temperatures," *Paris J. l'Ecole Polytech.*, vol. 1, cahier 22, pp. 24–76, 1795.
[52] R. Taghipour, T. Perez, and T. Moan, "Hybrid frequency time domain models for dynamic response analysis of marine structures," *Ocean Eng.*, vol. 35, no. 7, pp. 685–705, 2008.
[53] J. Shek, D. Macpherson, and M. Mueller, "Phase and amplitude control of a linear generator for wave energy conversion," in *Proc. 4th IET Conf. Power Electronics, Machines Drives*, 2008, pp. 66–70.
[54] A. Zurkinden, M. Guerinel, M. Alves, and L. Damkilde, "Theoretical investigation of a wave energy system by applying reactive control using stochastic analysis of the wave state," in *Proc. 11th European Wave Tidal Energy Conf.*, Aalborg, Denmark, 2013.
[55] W. Leithead and B. Connor, "Control of variable speed wind turbines: Design task," *Int. J. Control*, vol. 73, no. 13, pp. 1189–1212, 2000.
[56] S.-q. Qiu, J.-w. Ye, D.-j. Wang, and F.-l. Liang, "Experimental study on a pendulum wave energy converter," *China Ocean Eng.*, vol. 27, no. 3, pp. 359–368, 2013.
[57] B. Quine, J. Uhlmann, and H. Durrant-Whyte, "Implicit Jacobians for linearised state estimation in nonlinear systems," in *Proc. American Control Conf.*, 1995, pp. 1645–1646.
[58] K. Budal and J. Falnes, "The Norwegian wave-power buoy project," in *Proc. 2nd Int. Symp. Wave Energy Utilization*, 1982, pp. 323–344.
[59] F. Fusco and J. Ringwood, "Short-term wave forecasting for real-time control of wave energy converters," *IEEE Trans. Sust. Energy*, vol. 1, no. 2, pp. 99–106, 2010.
[60] M. Morari and Z. Evanghelos, *Robust Process Control*. Englewood Cliffs, NJ: Prentice-Hall, 1989.
[61] F. Fusco and J. Ringwood, "Hierarchical robust control of oscillating wave energy converters with uncertain dynamics," *IEEE Trans. Sust Energy*, vol. 5, no. 3, pp. 958–966, 2014.
[62] A. Price, C. Dent, and A. Wallace, "On the capture width of wave energy converters," *Appl. Ocean Res.*, vol. 31, no. 4, pp. 251–259, 2009.
[63] F. Fusco and J. Ringwood, "A simple and effective real-time controller for wave energy converters," *IEEE Trans. Sust. Energy*, vol. 4, no. 1, pp. 21–30, 2013.
[64] P. Kracht, "Wave prediction and its implementation on control systems of wave-energy converters," Fraunhofer IWES, EU MaRINet Infrastructure Access Report, Tech. Rep. MARINET-TA1-Adaptive WEC control, Sept. 2013.
[65] J. E. Cuthrell and L. T. Biegler, "On the optimization of differential-algebraic process systems," *AIChE J.*, vol. 33, no. 8, pp. 1257–1270, 1987.
[66] G. Bacelli, J. Ringwood, and J.-C. Gilloteaux, "A control system for a self-reacting point absorber wave energy converter subject to constraints," in *Proc. IFAC World Congr.*, 2011, pp. 11387–11392.
[67] G. Bacelli, "Control systems for wave energy devices," Ph.D. dissertation, Nat. Univ. Ireland, Maynooth, Ireland, 2014.
[68] J. Nocedal and S. J. Wright, *Numerical Optimization*, 2nd ed. New York: Springer-Verlag, 2006.
[69] J. Hals, J. Falnes, and T. Moan, "Constrained optimal control of a heaving buoy wave-energy converter," *J. Offshore Mech. Arct. Eng.*, vol. 133, pp. 011401.1–.15, Nov. 2010.
[70] J. Cretel, A. Lewis, G. Lightbody, and G. Thomas, "An application of model predictive control to a wave energy point absorber," in *Proc. IFAC Conf. Control Methodologies Technology Energy Efficiency*, 2010, pp. 267–272.
[71] G. Li and M. Belmont, "Model predictive control of an array of wave energy converters," in *Proc. 11th European Wave Tidal Energy Conf.*, Aalborg, Denmark, 2013.
[72] J. Scruggs, S. Lattanzio, A. Taflanidis, and I. Cassidy, "Optimal causal control of a wave energy converter in a random sea," *Appl. Ocean Res.*, vol. 42, pp. 1–15, Aug. 2013.
[73] S. H. Salter, "Wave power," *Nature*, vol. 249, no. 5459, pp. 720–724, 1974.
[74] D. V. Evans, "A theory for wave-power absorption by oscillating bodies," *J. Fluid Mech. Digital Arch.*, vol. 77, no. 1, pp. 1–25, 1976.
[75] D. V. Evans, "Power from water waves," *Annu. Rev. Fluid Mech.*, vol. 13, no. 1, pp. 157–187, Jan. 1981.
[76] C. C. Mei, "Power extraction from water waves," *J. Ship Res.*, vol. 20, pp. 63–66, June 1976.
[77] B. M. Count, "On the dynamics of wave-power devices," *Proc. Roy. Soc. London A, Math. Phys. Sci.*, vol. 363, no. 1715, pp. 559–579, 1978.
[78] I. Glendenning, "Wave energy," *Proc. Inst. Elec. Eng.*, vol. 127, pt. A, no. 5, pp. 301–307, 1980.
[79] J. Falnes, "A review of wave-energy extraction," *Marine Struct.*, vol. 20, no. 4, pp. 185–201, Oct. 2007.
[80] J. Falnes, "Optimum control of oscillation of wave-energy converters," in "Annex Report B1: Device Fundamentals/Hydrodynamics of the Wave Energy Converters: Generic Technical Evaluation Study," Inst. Fysikk, Univ. Trondheim, Trondheim, Norway, Tech. Rep., 1993.
[81] F. Farley, R. Rainey, and J. Chaplin, Eds., "The peaks and troughs of wave energy: The dreams and the reality," *Philos. Trans. Roy. Soc. A Math. Phys. Eng. Sci.*, vol. 370, no. 1959, pp. 201–529, Jan. 2012.
[82] M. Molinas, O. Skjervheim, P. Andreasen, T. Undeland, J. Hals, T. Moan, and B. Sorby, "Power electronics as grid interface for actively controlled wave energy converters," in *Proc. Int. Conf. Clean Electrical Power*, 2007, pp. 188–195.
[83] J. Hals, R. Taghipour, and T. Moan, "Dynamics of a force-compensated two-body wave energy converter in heave with hydraulic power takeoff subject to phase control," in *Proc. 7th European Wave Tidal Energy Conf.*, Porto, Portugal, Sept. 2007.
[84] T. Bjarte-Larsson and J. Falnes, "Investigation of phase-controlled wave-power buoy," in *Proc. 6th European Wave Tidal Energy Conf.*, Glasgow, U.K., 2005, pp. 47–50.
[85] J. Falnes and T. Bjarte-Larsson, "Theoretical and experimental investigation of wave energy conversion by a phase-controlled heaving body," *Proc. Inst. Mech. Eng. M*, vol. 220, no. 4, pp. 175–183, 2006.
[86] T. Bjarte-Larsson and J. Falnes, "Laboratory experiment on heaving body with hydraulic power take-off and latching control," *Ocean Eng.*, vol. 33, no. 7, pp. 847–877, 2006.
[87] A. F. d. O. Falcão, P. A. P. Justino, J. C. C. Henriques, and J. M. C. S. André, "Reactive versus latching phase control of a two-body heaving wave energy converter," in *Proc. European Control Conf.*, Uppsala, Sweden, 2009.
[88] P. Beirão, D. Valério, and J. S. da Costa, "Comparison of control strategies applied to the Archimedes wave swing," in *Proc. European Control Conf.*, Porto, Portugal, 2007.
[89] D. Valério, P. Beirão, and J. S. da Costa, "Optimisation of wave energy extraction with the Archimedes wave swing," *Ocean Eng.*, vol. 34, nos. 17–18, pp. 2330–2344, 2007.
[90] D. Valério, P. Beirao, M. Mendes, and J. S. da Costa, "Comparison of control strategies performance for a wave energy converter," in *Proc. 16th Mediterranean Conf. Control Automation*, 2008, pp. 773–778.
[91] J. Hals, J. Falnes, and T. Moan, "A comparison of selected strategies for adaptive control of wave energy converters," *J. Offshore Mech. Arct. Eng.*, vol. 133, no. 3, pp. 031101–031113, 2011.
[92] F. Fusco and J. Ringwood, "A study of the prediction requirements in real-time control of wave energy converters," *IEEE Trans. Sust. Energy*, vol. 3, no. 1, pp. 176–184, 2012.
[93] R. Hansen, "Design and control of the power take-off system for a wave energy converter with multiple absorbers," Ph.D. dissertation, Aalborg Univ., Aalborg, Denmark, 2014.
[94] D. Evans, "Some theoretical aspects of three-dimensional wave-energy absorbers," in *Proc. 1st Symp. Wave Energy Utilization*, Gothenburg, Sweden, 1979, pp. 78–112.
[95] J. Falnes, "Radiation impedance matrix and optimum power absorption for interacting oscillators in surface waves," *Appl. Ocean Res.*, vol. 2, no. 2, pp. 75–80, 1980.
[96] J. Falnes, "Principles for capture of energy from ocean waves. Phase control and optimum oscillation," Dept. Phys., NTNU Trondheim, Trondheim, Norway, Tech. Rep. N-7034, 1997.

[97] J. Falnes, "Optimum control of oscillation of wave-energy converters," in *Proc. 11th Int. Offshore Polar Engineering Conf.*, 2001.
[98] U. Korde, "Control system applications in wave energy conversion," in *Proc. OCEANS MTS/IEEE Conf. Exhibition*, 2000, vol. 3, pp. 1817–1824.
[99] S. H. Salter, "Power conversion systems for ducks," in *Proc. Int. Conf. Future Energy Concepts*, 1979, pp. 100–108.
[100] P. Nebel, "Maximising the efficiency of wave-energy plants using complex-conjugate control," *J. Syst. Control Eng.*, vol. 206, no. 4, pp. 225–236, 1992.
[101] J. Hals, T. Bjarte-Larsson, and J. Falnes, "Optimum reactive control and control by latching of a wave-absorbing semisubmerged heaving sphere," in *ASME Conf. Proc.*, 2002, pp. 415–423.
[102] J. Shek, D. Macpherson, M. Mueller, and J. Xiang, "Reaction force control of a linear electrical generator for direct drive wave energy conversion," *IET Renew. Power Gener.*, vol. 1, no. 1, pp. 17–24, 2007.
[103] U. A. Korde, "On providing a reaction for efficient wave energy absorption by floating devices," *Appl. Ocean Res.*, vol. 21, no. 5, pp. 235–248, 1999.
[104] U. A. Korde, "Systems of reactively loaded coupled oscillating bodies in wave energy conversion," *Appl. Ocean Res.*, vol. 25, no. 2, pp. 79–91, 2003.
[105] J. Falnes, "Wave-energy conversion through relative motion between two single-mode oscillating bodies," *J. Offshore Mech. Arct. Eng.*, vol. 121, no. 1, pp. 32–38, 1999.
[106] E. Tedeschi, M. Molinas, M. Carraro, and P. Mattavelli, "Analysis of power extraction from irregular waves by all-electric power take off," in *Proc. IEEE Energy Conversion Congr. Expo.*, 2010, pp. 2370–2377.
[107] E. Tedeschi, M. Carraro, M. Molinas, and P. Mattavelli, "Effect of control strategies and power take-off efficiency on the power capture from sea waves," *IEEE Trans. Energy Convers.*, vol. 26, no. 4, pp. 1088–1098, 2011.
[108] H. Yavuz, S. Mistikoglu, and T. Stallard, "Processing irregular wave measurements to enhance point absorber power capture performance," *Ocean Eng.*, vol. 38, no. 4, pp. 684–698, 2011.
[109] B. Li, D. E. Macpherson, and J. K. H. Shek, "Direct drive wave energy converter control in irregular waves," in *Proc. IET Conf. Renewable Power Generation*, 2011, pp. 1–6.
[110] B. Li, R. Crozier, and E. Macpherson, "Reactive causal control of a linear generator in irregular waves for wave power system," in *Proc. 9th European Wave Tidal Energy Conf.*, Southampton, U.K., 2011.
[111] D. M. Andrade, A. G. Santana, and A. de la Villa Jaen, "Frequency-matching assessment under reactive control on wave energy converters," in *Proc. 4th Int. Conf. Ocean Energy*, Dublin, Ireland, 2012.
[112] R. H. Hansen and M. M. Kramer, "Modelling and control of the Wavestar prototype," in *Proc. 9th European Wave Tidal Energy Conf.*, 2011, pp. 1–10.
[113] F. Fusco and J. V. Ringwood, "Suboptimal causal reactive control of wave energy converters using a second order system model," in *Proc. 21st Int. Offshore Polar Engineering Conf.*, 2011, pp. 687–694.
[114] S. Lattanzio and J. Scruggs, "Maximum power generation of a wave energy converter in a stochastic environment," in *Proc. IEEE Int. Conf. Control Applications*, 2011, pp. 1125–1130.
[115] J. Scruggs and S. Lattanzio, "Optimal causal control of an ocean wave energy converter in stochastic waves," in *Proc. 9th European Wave Tidal Energy Conf.*, 2011, pp. 1–6.
[116] S. R. Nielsen, Q. Zhou, M. M. Kramer, B. Basu, and Z. Zhang, "Optimal control of nonlinear wave energy point converters," *Ocean Eng.*, vol. 72, pp. 176–187, Nov. 2013.
[117] M. Vantorre, R. Banasiak, and R. Verhoeven, "Modelling of hydraulic performance and wave energy extraction by a point absorber in heave," *Appl. Ocean Res.*, vol. 26, no. 1–2, pp. 61–72, 2004.
[118] G. de Backer, M. Vantorre, R. Banasiak, J. de Rouck, C. Beels, and H. Verhaeghe, "Performance of a point absorber heaving with respect to a floating platform," in *Proc. 7th European Wave Tidal Energy Conf.*, Porto, Portugal, 2007.
[119] H. Yavuz, T. J. Stallard, A. P. McCabe, and G. A. Aggidis, "Time series analysis-based adaptive tuning techniques for a heaving wave energy converter in irregular seas," *Proc. Inst. Mech Eng. Part A J. Power Energy*, vol. 221, no. 1, pp. 77–90, 2007.
[120] J. A. Oskamp and H. T. Ozkan-Haller, "Power calculations for a passively tuned point absorber wave energy converter on the Oregon coast," *Renew. Energy*, vol. 45, pp. 72–77, Sept. 2012.
[121] A. de Andros, R. Guanche, J. Armesto, F. del Jesus, C. Vidal, and I. Losada, "Time domain model for a two-body heave converter: Model and applications," *Ocean Eng.*, vol. 72, pp. 116–123, Nov. 2013.
[122] R. Waters, M. Stalberg, O. Danielsson, O. Svensson, S. Gustafsson, E. Stromstedt, M. Eriksson, J. Sundberg, and M. Leijon, "Experimental results from sea trials of an offshore wave energy system," *Appl. Phys. Lett.*, vol. 90, no. 3, pp. 034105–034105-3, 2007.
[123] M. Eriksson, R. Waters, O. Svensson, J. Isberg, and M. Leijon, "Wave power absorption: Experiments in open sea and simulation," *J. Appl. Phys.*, vol. 102, no. 8, pp. 084910–084910-5, 2007.
[124] J. Engström, V. Kurupath, J. Isberg, and M. Leijon, "A resonant two body system for a point absorbing wave energy converter with direct-driven linear generator," *J. Appl. Phys.*, vol. 110, no. 12, pp. 124904–124915, 2011.
[125] M. Stalberg, R. Waters, O. Danielsson, and M. Leijon, "Influence of generator damping on peak power and variance of power for a direct drive wave energy converter," *J. Offshore Mech. Arct. Eng.*, vol. 130, no. 3, pp. 031003–4, 2008.
[126] C. Bostrom, R. Waters, E. Lejerskog, O. Svensson, M. Stalberg, E. Stromstedt, and M. Leijon, "Study of a wave energy converter connected to a nonlinear load," *IEEE J. Ocean. Eng.*, vol. 34, no. 2, pp. 123–127, 2009.
[127] K. Schlemmer, F. Fuchshumer, N. Bohmer, R. Costello, and C. Villegas, "Design and control of a hydraulic power take-off for an axisymmetric heaving point absorber," in *Proc. 9th European Wave Tidal Energy Conf.*, Southampton, U.K., 2011.
[128] C. Cargo, "Optimal design of a WEC hydraulic power take-off unit in irregular waves," in *Proc. 9th European Wave Tidal Energy Conf.*, Southampton, U.K., 2011.
[129] C. J. Cargo, A. R. Plummer, A. J. Hillis, and M. Schlotter, "Determination of optimal parameters for a hydraulic power take-off unit of a wave energy converter in regular waves," *Proc. Inst. Mech. Eng. A, J. Power Energy*, vol. 226, no. 1, pp. 98–111, 2012.
[130] P. Beirão, M. J. G. C. Mendes, D. Valério, and J. S. da Costa, "Control of the Archimedes wave swing using neural networks," in *Proc. 7th European Wave Tidal Energy Conf.*, Porto, Portugal, 2007.
[131] D. Valério, M. J. Mendes, P. Beirio, and J. S. da Costa, "Identification and control of the AWS using neural network models," *Appl. Ocean Res.*, vol. 30, no. 3, pp. 178–188, 2008.
[132] A. F. de O. Falcão, "Modelling and control of oscillating-body wave energy converters with hydraulic power take-off and gas accumulator," *Ocean Eng.*, vol. 34, nos. 14–15, pp. 2021–2032, 2007.
[133] G. Duclos, A. Babarit, and A. H. Clement, "Optimizing the power take off of a wave energy converter with regard to the wave climate," *J. Offshore Mech. Arct. Eng.*, vol. 128, no. 1, pp. 56–64, 2006.
[134] M. P. Schoen, J. Hals, and T. Moan, "Wave prediction and fuzzy logic control of wave energy converters in irregular waves," in *Proc. 16th Mediterranean Conf. Control Automation*, 2008, pp. 767–772.
[135] M. P. Schoen, J. Hals, and T. Moan, "Robust control of heaving wave energy devices in irregular waves," in *Proc. 16th Mediterranean Conf. Control Automation*, 2008, pp. 779–784.
[136] M. P. Schoen, J. Hals, and T. Moan, "Wave prediction and robust control of heaving wave energy devices for irregular waves," *IEEE Trans. Energy Convers.*, vol. 26, no. 2, pp. 627–638, 2011.
[137] T. R. Mundon, A. F. Murray, and R. Wallace, "Toward a biologically inspired, neural control mechanism for multiple degree of freedom wave energy converters," in *Proc. 9th European Wave Tidal Energy Conf.*, Uppsala, Sweden, 2011.
[138] K. Ahn, D. Truong, H. H. Tien, and J. I. Yoon, "An innovative design of wave converter," *Renew. Energy*, vol. 42, pp. 186–194, June 2012.
[139] E. Ozkop, I. Altas, and A. Sharaf, "A novel fuzzy logic tan-sigmoid controller for wave energy converter-grid interface DC energy utilization farm," in *Proc. Canadian Conf. Electrical Computer Engineering*, 2009, pp. 1184–1187.
[140] A. Sharaf and A. El-Gammal, "Optimal variable structure self regulating PSO-controller for stand-alone wave energy conversion scheme," in *Proc. 4th Asia Int. Conf. Mathematical/Analytical Modelling Computer Simulation*, 2010, pp. 438–443.
[141] J. J. Cândido and P. A. P. Justino, "Frequency, stochastic and time domain models for an articulated wave power device," in *Proc. ASME Conf.*, 2008, pp. 633–643.
[142] J. J. Candido and P. A. P. S. Justino, "Stochastic, time domain models and Pontryagin maximum principle for a two body wave power device," in *Proc. 8th European Wave Tidal Energy Conf.*, Uppsala, Sweden, 2009.
[143] C. J. Taylor, M. A. Stables, P. Cross, K. Gunn, and G. A. Aggidis, "Linear and nonlinear modeling and control of a power take-off simulation for wave energy conversion," in *Proc. 8th European Wave Tidal Energy Conf.*, Uppsala, Sweden, 2009.
[144] P. Cross, C. J. Taylor, and G. A. Aggidis, "State dependent feed-forward control for wave energy conversion," in *Proc. 9th European Wave Tidal Energy Conf.*, Southampton, U.K., 2011.

[145] K. Gunn, C. J. Taylor, and C. Lingwood, "Evolutionary algorithms for the development and optimisation of wave energy converter control systems," in *Proc. 8th European Wave Tidal Energy Conf.*, Uppsala, Sweden, 2009.
[146] P. Ricci, J. Lopez, M. Santos, J. L. Villate, P. Ruiz-Minguela, F. Salcedo, and A. F. de O. Falcao, "Control strategies for a simple point-absorber connected to a hydraulic power take-off," in *Proc. 8th European Wave Tidal Energy Conf.*, Uppsala, Sweden, 2009.
[147] P. Ricci, J. Lopez, M. Santos, P. Ruiz-Minguela, J. Villate, F. Salcedo, and A. de O. Falcão, "Control strategies for a wave energy converter connected to a hydraulic power take-off," *IET Renew. Power Gener.*, vol. 5, no. 3, pp. 234–244, 2011.
[148] R. Costello, J. V. Ringwood, and J. Webber, "Comparison of two alternative hydraulic PTO concepts for wave energy conversion," in *Proc. 9th European Wave Tidal Energy Conf.*, Southampton, U.K., 2011.
[149] R. Hansen, T. Andersen, and H. Pedersen, "Comparison of reactive and non-reactive control strategies for wave energy converters with non-ideal power take-off systems," *Renew. Energy*, to be published.
[150] E. Amon, A. Schacher, and T. Brekken, "A novel maximum power point tracking algorithm for ocean wave energy devices," in *Proc. IEEE Energy Conversion Congr. Expo.*, 2009, pp. 2635–2641.
[151] B. Orazov, O. O'Reilly, and Ö. Savas, "On the dynamics of a novel ocean wave energy converter," *J. Sound Vib.*, vol. 329, no. 24, pp. 5058–5069, 2010.
[152] P. R. Costa, P. B. Garcia-Rosa, and S. F. Estefen, "Phase control strategy for a wave energy hyperbaric converter," *Ocean Eng.*, vol. 37, nos. 17–18, pp. 1483–1490, 2010.
[153] T. Lewis, A. von Jouanne, and T. Brekken, "Wave energy converter with wideband power absorption," in *Proc. IEEE Energy Conversion Congr. Expo.*, 2011, pp. 3844–3851.
[154] M. R. Belmont, "A lower bound estimate of the gains stemming from quiescent period predictive control using conventional sea state statistics," *J. Renew. Sust. Energy*, vol. 1, no. 6, p. 063104, 2009.
[155] M. Belmont, "Increases in the average power output of wave energy converters using quiescent period predictive control," *Renew. Energy*, vol. 35, no. 12, pp. 2812–2820, 2010.
[156] J. Newman, "Absorption of wave energy by elongated bodies," *Appl. Ocean Res.*, vol. 1, no. 4, pp. 189–196, 1979.
[157] D. Evans, "Maximum wave-power absorption under motion constraints," *Appl. Ocean Res.*, vol. 3, no. 4, pp. 200–203, 1981.
[158] D. Pizer, "Maximum wave-power absorption of point absorbers under motion constraints," *Appl. Ocean Res.*, vol. 15, no. 4, pp. 227–234, 1993.
[159] U. Korde, "Use of oscillation constraints in providing a reaction for deep water floating wave energy devices," *Int. J. Offshore Polar Eng.*, vol. 11, no. 2, pp. 1473–1484, 2001.
[160] G. de Backer, "Hydrodynamic design optimization of wave energy converters consisting of heaving point absorbers," Ph.D. dissertation, Faculty Eng., Ghent Univ., Ghent, Belgium, 2009.
[161] J. Scruggs, "Multi-objective optimal causal control of an ocean wave energy converter in random waves," in *Proc. OCEANS*, 2011, pp. 1–6.
[162] H. Eidsmoen, "Optimum control of a floating wave-energy converter with restricted amplitude," *J. Offshore Mech. Arct. Eng.*, vol. 118, no. 2, pp. 96–102, 1996.
[163] J. Hals, J. Falnes, and T. Moan, "Constrained optimal control of a heaving buoy wave-energy converter," *J. Offshore Mech. Arct. Eng.*, vol. 133, no. 1, p. 011401, 2011.
[164] J. A. M. Cretel, G. Lightbody, G. P. Thomas, and A. W. Lewis, "Maximisation of energy capture by a wave-energy point absorber using model predictive control," in *Proc. IFAC World Congr.*, 2011, pp. 3714–3721.
[165] T. Brekken, "On model predictive control for a point absorber wave energy converter," in *Proc. IEEE PowerTech*, Trondheim, Norway, 2011, pp. 1–8.
[166] M. Richter, M. Magana, O. Sawodny, and T. Brekken, "Nonlinear model predictive control of a point absorber wave energy converter," *IEEE Trans. Sust. Energy*, vol. 4, no. 1, pp. 118–126, 2013.
[167] G. Li and M. R. Belmont, "Model predictive control of sea wave energy converters–Part I: A convex approach for the case of a single device," *Renew. Energy*, vol. 69, pp. 453–463, 2014.
[168] N. Tom and R. W. Yeung, "Non-linear model predictive control applied to a generic ocean-wave energy extractor," in *Proc. 32nd Int. Conf. Ocean, Offshore Arctic Engineering*, Nantes, France, 2013.
[169] J. Falnes and K. Budal, "Wave-power absorption by parallel rows of interacting oscillating bodies," *Appl. Ocean Res.*, vol. 4, no. 4, pp. 194–207, 1982.
[170] J. Falnes, "Wave-power absorption by an array of attenuators oscillating with unconstrained amplitudes," *Appl. Ocean Res.*, vol. 6, no. 1, pp. 16–22, 1984.
[171] C. Fitzgerald and G. P. Thomas, "A preliminary study of the optimal formation of an array of wave power devices," in *Proc. 7th European Wave Tidal Energy Conf.*, Porto, Portugal, 2007.
[172] P. A. Justino and A. Clément, "Hydrodynamic performance for small arrays of submerged spheres," in *Proc. 5th European Wave Tidal Energy Conf.*, 2003, pp. 266–273.
[173] A. Z. Annuar, D. E. Macpherson, D. I. M. Forehand, and M. A. Mueller, "Optimum power control for arrays of direct drive wave energy converters," in *Proc. 6th IET Int. Conf. Power Electronics, Machines Drives*, 2012, pp. 1–6.
[174] P. Ricci, J.-B. Saulnier, and A. F. de O. Falcao, "Point-absorber arrays: A configuration study off the Portuguese west-coast," in *Proc. 7th European Wave Tidal Energy Conf.*, Porto, Portugal, 2007.
[175] J. Cruz, R. Sykes, P. Siddorn, and R. E. Taylor, "Wave farm design: Preliminary studies on the influences of wave climate, array layout and farm control," in *Proc. 8th European Wave Tidal Energy Conf.*, 2009, pp. 736–745.
[176] J. Cruz, R. Sykes, P. Siddorn, and R. Taylor, "Estimating the loads and energy yield of arrays of wave energy converters under realistic seas," *IET Renew. Power Gener.*, vol. 4, no. 6, pp. 488–497, 2010.
[177] R. Antonutti and G. E. Hearn, "Optimisation of point-absorber arrays," in *Proc. 9th European Wave Tidal Energy Conf.*, Southampton, U.K., 2011.
[178] B. Child and V. Venugopal, "Non-optimal tuning of wave energy device arrays," in *Proc. 2nd Int. Conf. Ocean Energy*, Brest, France, 2008.
[179] B. Child and V. Venugopal, "Optimal configurations of wave energy device arrays," *Ocean Eng.*, vol. 37, no. 16, pp. 1402–1417, 2010.
[180] P. C. Vicente, A. F. de O. Falcão, and P. A. Justino, "A time domain analysis of arrays of floating point-absorber wave energy converters including the effect of nonlinear mooring forces," in *Proc. 3rd Int. Conf. Ocean Energy*, Bilbao, Spain, 2010.
[181] B. Borgarino, A. Babarit, and P. Ferrant, "Impact of wave interactions effects on energy absorption in large arrays of wave energy converters," *Ocean Eng.*, vol. 41, pp. 79–88, Feb. 2012.
[182] S. Bellew, T. Stallard, and P. Stansby, "Optimisation of a heterogeneous array of heaving bodies," in *Proc. 8th European Wave Tidal Energy Conf.*, Uppsala, Sweden, 2009.
[183] G. De Backer, M. Vantorre, C. Beels, J. De Rouck, and P. Frigaard, "Performance of closely spaced point absorbers with constrained floater motion," in *Proc. 8th European Wave Tidal Energy Conf.*, 2009, pp. 806–817.
[184] G. De Backer, M. Vantorre, C. Beels, J. De Rouck, and P. Frigaard, "Power absorption by closely spaced point absorbers in constrained conditions," *IET Renew. Power Gener.*, vol. 4, no. 6, pp. 579–591, 2010.
[185] A. Babarit, B. Borgarino, P. Ferrant, and A. Clement, "Assessment of the influence of the distance between two wave energy converters on energy production," *IET Renew. Power Gener.*, vol. 4, no. 6, pp. 592–601, 2010.
[186] A. Price and A. Wallace, "Non-linear methods for next wave estimation," in *Proc. 7th European Wave Tidal Energy Conf.*, Porto, Portugal, 2007.
[187] J. Eder, J. Bretl, and K. Edwards, "Empirical demonstration of acausal-control strategies for wave energy converters," in *Proc. 32nd Int. Conf. Ocean, Offshore Arctic Engineering*, Nantes, France, 2013, p. V008T09A001.
[188] K. Monk, D. Conley, M. Lopez, and Q. Zou, "Pneumatic power regulation by wave forecasting and real-time relief valve control for an OWC," in *Proc. 11th European Wave Tidal Energy Conf.*, Aalborg, Denmark, 2013.
[189] U. A. Korde, "On a near-optimal control approach for a wave energy converter in irregular waves," *Appl. Ocean Res.*, vol. 46, pp. 79–93, 2014.
[190] F. Paparella, K. Monk, V. Winands, M. Lopes, D. Conley, and J. Ringwood, "Benefits of up-wave measurements in linear short-term wave forecasting for wave energy applications," in *Proc. IEEE Multi-Conf. Systems Control*, Antibes, France, 2014.
[191] J.-C. Gilloteaux and J. Ringwood, "Control-informed geometric optimisation of wave energy converters," in *Proc. IFAC Conf. Control Applications Marine Systems*, 2010, pp. 399–404.
[192] P. Garcia-Rosa, G. Bacelli, and J. Ringwood, "Control-informed optimal array layout for wave farms," *IEEE Trans. Sust. Energy*, to be published 2014.
[193] R. Costello, B. Teillant, J. Weber, and J. Ringwood, "Techno-economic optimisation for wave energy converters," in *Proc. Int. Conf. Ocean Energy*, Dublin, Ireland, 2012.
[194] B. Teillant, R. Costello, J. Weber, and J. Ringwood, "Productivity and economic assessment of wave energy projects through operational simulations," *Renew. Energy*, vol. 48, pp. 220–230, 2012.